https://doi.org/10.5194/gmd-2020-248
Preprint. Discussion started: 8 January 2021

Geoscientific Model Development Discussions

THE ENEA-REG SYSTEM (v1.0), A MULTI-COMPONENT REGIONAL EARTH SYSTEM MODEL. SENSITIVITY TO DIFFERENT ATMOSPHERIC COMPONENTS OVER MED-CORDEX REGION

Alessandro Anav[1], Adriana Carillo[1], Massimiliano Palma[1], Maria Vittoria Struglia[1], Ufuk Utku Turuncoglu[2], Gianmaria Sannino[1]

[1] Italian National Agency for New Technologies, Energy and the Environment (ENEA), Rome, Italy.

[2] National Center for Atmospheric Research, Boulder, CO, USA

Abstract

In this study, a new regional Earth system model is developed and applied to the Med-CORDEX region. The ENEA-REG system is made up of two interchangeable regional climate models as atmospheric components (RegCM and WRF), a river model (HD), and an ocean model (MITgcm); processes taking place at the land surface are represented within the atmospheric models with the possibility to use several land surface schemes of different complexity. The coupling between these components is performed through the RegESM driver.

Here, we present and describe our regional Earth system model and evaluate its components using a multidecadal hindcast simulation over the period 1980-2013 driven by ERA-INTERIM reanalysis. We show how the atmospheric components are able to correctly reproduce both large-scale and local features of the Euro-Mediterranean climate, although some remarkable biases are relevant for some variables. In particular, WRF has a significant cold bias during winter over North-Eastern bound of the domain, while RegCM systematically overestimates the wind speed over the Mediterranean Sea. This latter bias has severe consequences on the ocean component: we show that when WRF is used as the atmospheric component of the Earth system, the performances of the ocean model are remarkably better compared with the RegCM version.

Our regional Earth system model allows studying the Euro-Mediterranean climate system and can be applied to both hindcast and scenario simulations.

https://doi.org/10.5194/gmd-2020-248
Preprint. Discussion started: 8 January 2021

Geoscientific Model Development Discussions

1. Introduction

The Mediterranean basin is a complex region, characterized by the presence of pronounced topography and a complex land-sea distribution including a considerable number of islands and several straits. These features generate strong local atmosphere–sea interactions leading to the formation of intense local winds, like Mistral, Etesian and Bora which, in turn, dramatically affect the Mediterranean ocean circulation (e.g. Artale et al., 2010; Lebeaupin-Brossier et al. 2015; Turuncoglu and Sannino, 2017). Given the relatively fine spatial scales at which these processes take place, the Mediterranean basin provides a good opportunity to study regional climate, with a special focus on the air-sea coupling (Sevault et al., 2014; Turuncoglu and Sannino, 2017). For these reasons, regional coupled models have been developed and used to study both present and future Mediterranean climate system (e.g. Dubois et al., 2012; Ruti el al., 2016; Darmaraki et al., 2019; Parras-Berrocal et al., 2020); these models, depending on their complexity, include several physical components of the climate system, like atmosphere, ocean, land surface, rivers and biogeochemistry (both for land and ocean) (e.g. Drobinski et al., 2012; Sevault et al., 2014; Reale et al., 2020). Since the last two decades, an increasing number of studies have been performed over the Mediterranean basin and nowadays there is a coordinated effort for producing hindcast and future simulations over this region using regional coupled climate models sharing some common protocols (Ruti el al., 2016). In particular, the Coordinated Regional Climate Downscaling Experiment (CORDEX) was designed to produce, worldwide, high-resolution regional climate simulations through a coordinated experiment protocol ensuring that model simulations are carried out under similar conditions facilitating thus the analysis, intercomparison, and synthesis of different simulations (Giorgi et al., 2015; Giorgi et al., 2016). In the framework of the CORDEX program, regional climate model simulations dedicated to the Mediterranean area belong to the Med-CORDEX initiative (Ruti el al., 2016, Somot et al., 2018).

From an atmospheric point of view, the Mediterranean region is a transition zone between arid subtropics and temperate mid-latitudes, characterized by low annual precipitation totals and high interannual variability; during winter, rain is brought by mid-latitude westerlies, while warm and dry summer results from the influence of subtropical remote forcing triggered by the Indian monsoon (Tuel and Eltahir, 2020). Future model projections have indicated that the

https://doi.org/10.5194/gmd-2020-248
Preprint. Discussion started: 8 January 2021


Geoscientific Model Development Discussions

Mediterranean is expected to be one of the most prominent and vulnerable climate change "hotspots" in the world; in particular, a significant decline in the amount of precipitation is predicted by several models over the twenty-first century (Giorgi 2006; Tuel and Eltahir, 2020). Given the complexity of the Mediterranean basin and the strong air–sea feedback, high resolution regional Earth system models are an optimal tool for accurate simulation of past, present and future climate over this region. The main aims of this paper are to present and evaluate the newly developed regional Earth system model ENEA-REG; in particular, we perform the evaluation run of the ENEA-REG system making a hindcast simulation using the ERA-interim reanalysis as boundary conditions. The performances of individual model components are evaluated comparing results with a wide range of observation-based datasets. Taking full advantage of the potential offered by the RegESM coupler (Turuncoglu 2019), that allows to build up in a modular way regional coupled models, the ENEA-REG is composed of two interchangeable regional climate models used as atmospheric components of the Earth system. Keeping fixed the ocean and rivers components, our model allows to explore the sensitivity of the ocean model to different atmospheric forcings: specifically, with the direct comparison of simulations differing for the atmospheric component, we infer the impact of different modeling choices on both air-sea processes and, consequently, on the ocean dynamics. Our results help to define possible future modelling strategies.

2. Model description

2.1 The RegESM coupler

The ENEA-REG regional Earth system model has the capability to include several model components (atmosphere, river routing, ocean, wave) to allow different modeling applications.For each simulation, the components of the modeling system can be easily enabled or disabled via the driver's configuration file. In addition, the modeling framework also supports plugging new earth system sub-components (e.g. atmospheric chemistry, sea ice, ocean biogeochemistry) with minimal code changes through its simplified interface, which is called "cap". TheNational United Operational Prediction Capability (NUOPC) cap is a Fortran module that serves as interface to a model when it is used in a NUOPC-based coupled system;it is a small software layer that sits on top of a model code, making calls into it and exposing model data structures in a standard way (Turuncoglu, 2019).

https://doi.org/10.5194/gmd-2020-248
Preprint. Discussion started: 8 January 2021


Geoscientific Model Development Discussions

In this study, the modeling system is configured to include three components: a regional atmospheric climate model, a regional ocean model and an hydrological model. The driver used to glue, regrid and exchange data among the three components of ENEA-REG modeling system is RegESM (Turuncoglu 2019). The driver employs the Earth System Modeling Framework (ESMF) library (version 7.1) and the NUOPC layer to connect and synchronize each model component and perform interpolation among different horizontal grids (Turuncoglu 2019). While the ESMF library deals with interpolation and regridding of exchanged fields, the NUOPC layer simplifies common tasks of model coupling like component synchronization and run sequence by providing additional wrapper layer between coupled model and ESMF framework (Turuncoglu and Sannino, 2017; Turuncoglu 2019). It also allows defining different coupling time intervals among the components to reproduce fast and slow interactions among the model components (Turuncoglu and Sannino, 2017; Turuncoglu 2019). In this study, the model coupling time step between ocean and atmosphere is set to 3-hours, while the coupling with the hydrological model is defined as 1-day. In addition, the driver allows selecting the desired exchange fields from a simple field database containing all available variables that can be exported or imported by the different components. In this way, the coupled modeling system can be easily adapted depending on the application and the particular configuration of the experiment without any code customizations in both the driver and individual model components (Turuncoglu, 2019).

In the experiment presented here, the atmospheric model retrieves sea surface temperature (SST) from the ocean model (where grids are overlapped), while the ocean model collects surface pressure, wind components, freshwater (evaporation-precipitation, i.e. E-P) and heat fluxes from the atmospheric component. Similarly, the hydrological model uses surface and sub-surface runoff simulated by the atmospheric component to compute the river drainage and exchanges this field with the ocean component to close the water cycle. Further details on the ENEA-REG framework and the interaction among the components are schematically depicted in **Figure 1**.

In the current work, we performed hindcast simulations covering the period 1st October 1979-31st December 2013.

2.2 The atmospheric components: WRF and RegCM

https://doi.org/10.5194/gmd-2020-248
Preprint. Discussion started: 8 January 2021


Geoscientific Model Development Discussions

The ENEA-REG regional Earth system model is made up of two interchangeable atmospheric components: the Weather Research and Forecasting (WRF; Skamarock et al., 2008) model and the REGional Climate Model (RegCM; Giorgi et al., 2012).

WRF is a limited-area, non-hydrostatic, terrain-following eta-coordinate mesoscale model developed by the NCAR/MMM (National Center for Atmospheric Research, Mesoscale and Microscale Meteorology division). WRF offers multiple options for various physical parameterizations, thus it can be used to any region of the world for a wide range of applications ranging from operational forecasts to realistic and idealized dynamical studies. In this work we use the dynamical core ARW (Advanced Research WRF, version 3.8.1) (Skamarock et al., 2008), with a single-moment 5 class scheme to resolve the microphysics (Hong et al., 2006) and the Rapid Radiative Transfer Model for GCMs (RRTMG) for the shortwave and longwave radiation (Iacono et al., 2008). Convective precipitation and cumulus parameterization are resolved via the Kain-Fritsch scheme (Kain 2004), the planetary boundary layer (PBL) is represented through the Yongsei University scheme (Hong et al., 2006), while the exchange of heat, water and momentum between soil-vegetation and atmosphere is simulated by Noah–MP land surface model(Niu et al, 2011). The model domain is projected on a Lambert conformal grid with a horizontal resolution of 15 km and with 35 vertical levels extending from land surface up to 50 hPa (**Figure 2a**). The initial and boundary meteorological conditions are provided by the European Centre for Medium-Range Weather Forecast (ECMWF) reanalysis (Dee et al., 2011) with a horizontal resolution of 0.75° every 6 h. The lateral buffer zone has a width of 10 grid points and uses an exponential relaxation to provide the model with lateral boundary conditions. In addition, we applied spectral nudging to temperature, wind components and moisture content above the PBL; nudging is conducted every 6 h, consistent with the frequency of ERA-Interim reanalysis data. A synthesis of parameterizations and input data used in this study is given in **Table 1**.

The other supported atmospheric component of the regional Earth system model is RegCM (version 4.5) a hydrostatic, compressible, sigma-p vertical coordinate model initially developed by Giorgi (1990) and Giorgi et al. (1993a, 1993b) and then modified as discussed by Giorgi et al. (2012); RegCM is maintained by ICTP's Earth System Physics (ESP) section. The dynamical core of RegCM is based on the primitive equations, hydrostatic version of the National Centre for Atmospheric Research (NCAR) and Pennsylvania State University mesoscale model MM5

https://doi.org/10.5194/gmd-2020-248
Preprint. Discussion started: 8 January 2021


Geoscientific Model Development Discussions

(Grell et al., 1994). Similar to WRF, RegCM includes different physics and sub-grid parameterization options. In this study, radiation is simulated with the radiative transfer scheme of the global model CCM3 (Kiehl 1996), cumulus convection is resolved through the Grell scheme (Grell 1993) with a Fritsch-Chappell scheme for unresolved convection, the planetary boundary layer is represented viaa modified version of the Holtslag parameterization (Giorgi et al 2012), while the exchange of heat, water and momentum between soil-vegetation and atmosphere is simulated by the Biosphere-Atmosphere Transfer Scheme (BATS) (Dickinson et al., 1993). The resolved scale precipitation is modeled with the SUBEX parameterization (Pal et al, 2000).

The model domain (**Figure 2b**) is projected on a Lambert conformal grid with a horizontal resolution of 20 km and with 23 vertical levels extending from land surface up to 50 hPa. Similarly to WRF, we used ERA-Interim data to force RegCM and 6 grid-points in each side are selected as relaxation zone with an exponentially decreasing relaxation coefficient (Giorgi et al. 1993) (**Table 1**).

A few modifications have been made both in WRF and RegCM to receive the oceanic surface variables and send the atmospheric fields to the ocean component of the ENEA-REG system, as described in **Figure 1**. Further details on the model's changes are described by Turuncoglu (2019).

2.3 The ocean component: MITgcm

The ocean component of the ENEA-REG system is the Massachusetts Institute of Technology General Circulation Model (MITgcm version c65; Marshall et al., 1997). The MITgcm solves both the hydrostatic and nonhydrostatic Navier-Stokes equations under the Boussinesq approximation for an incompressible fluid with a spatial finite-volume discretization on a curvilinear computational grid using the z* rescaled height vertical coordinate (Adcroft and Campin, 2004). MITgcm is designed to run on different platforms, from scalar to high-performance computing (HPC) systems: it is parallelized via MPI through a horizontal domain decomposition technique.

MITgcm is used by a broad community of researchers for a wide range of applications at various spatial and temporal scales ranging from local/regional (e.g. Sannino et al., 2009; Furue et al., 2015; Rosso et al., 2015; Sannino et al., 2015; McKiver et al., 2016; Sannino et al., 2017; Llasses

https://doi.org/10.5194/gmd-2020-248
Preprint. Discussion started: 8 January 2021


Geoscientific Model Development Discussions

et al 2018; Peng et al., 2019) to global ocean simulations (e.g. Stammer et al., 2003; Forget et al., 2015; Breitkreuz et al., 2018; Forget and Ferreira, 2019), including climate studies with MITgcm coupled to atmosphere (e.g. Artale et al., 2010; Polkova et al., 2014; Sitz et al., 2017; Sun et al., 2019).

In the configurations presented here, the MITgcm has been used in its hydrostatic, implicit free-surface, partial step topography formulation (Adcroft et al, 1997) and has already been customized and applied for simulating the Mediterranean circulation (Di Biagio et al 2019, Cusinato et al. 2018). The model domain has a horizontal resolution of 1/12°, corresponding to 570x264 grid points, and covers the entire Mediterranean Sea with the boundary conditions in the Atlantic Ocean (**Figure 2**). In the vertical the model is discretized using 75 unevenly spaced Z-levels going from 1 m at the surface to about 300 m in the deepest part of the basin. We use lateral open boundary conditions prescribed by the MITgcm Open Boundary Conditions (OBCS) package. Temperature and salinity boundary conditions in the Atlantic Ocean are interpolated from the global LEVITUS94 climatological monthly 3D data.

To ensure numerical stability a sponge layer is added to the open boundary of the domain. Each variable is then relaxed toward the boundary values with a relaxation timescale that decreases linearly with distance from the boundary. The thickness of the sponge layer in terms of grid points is 18 and inner fields are relaxed toward boundary values using a 10 day period. Salinity and temperature fields in the Mediterranean basin have been initialized using MEDATLAS/2002 climatology for the month of October. This month corresponds to a situation of stable vertical stratification and can avoid sudden vertical mixing. A spin up procedure for the ocean model has not been adopted, as in the regional ocean modeling community, the length of a spin-up is still a matter of debate. Usually, for climate studies, long spin-up are desirable to avoid the models drift considerably from the initial conditions and tend to converge toward a new state given by the ocean physics (Sitz et al., 2017); as the aim of this study is the comparison of two coupled model systems having in common the same ocean model, the MITgcm has the same initial and boundary conditions in its two configurations.

Similar to the atmospheric models, we have modified the MITgcm model in order to be forced by meteorological conditions derived by the atmospheric components of the ENEA-REG system (see Turuncoglu and Sannino 2017 for further details).

2.4 The river routing model: HD

https://doi.org/10.5194/gmd-2020-248
Preprint. Discussion started: 8 January 2021

The river discharge is a key variable in the Earth system modeling as it closes the water cycle between the atmosphere and ocean. The ENEA-REG system uses the Hydrological Discharge (HD, version 1.0.2) model, developed by the Max Planck Institute (Hagemann and Dümenil, 1998; Hagemann and Dümenil-Gates, 2001), to simulate freshwater fluxes over the land surface and to provide a river discharge to the ocean model. The HD model uses a regular global grid with a fixed horizontal resolution of 0.5° and it is forced by daily surface runoff and drainage data. Similarly to other components, the HD model was slightly modified (Turuncoglu and Sannino 2017) to retrieve surface runoff and drainage from the atmospheric components of the regional coupled model and to provide the river discharge to the ocean component (**Figure 1**).

3. Experiment design and observational datasets

In this work we present MED-CORDEX hindcast climate simulations performed with the ENEA-REG model using both the atmospheric components of the system (i.e. WRF and RegCM). Despite the simulations start time is October 1979, here we perform the model validation over the period 1982-2013, using the first 2 years of simulation as spin up to initialize all the fields of the different components of the coupled system. The validation of the coupled model focuses on sea surface temperature, sea surface salinity and mixed layer depth for the ocean, and 2m temperature, wind speed and freshwater and heat fluxes for the atmosphere. We also compare river discharge from Po river as it influences the circulation of Adriatic Sea and the formation of deep waters.

The simulated SST data are validated against the Objectively Interpolated Sea Surface Temperatures (OISST v2, Reynolds et al., 2002, 2007), developed and distributed by the National Oceanic and Atmospheric Administration (NOAA). The OISST composites observations from different platforms (satellites, ships, buoys) on a 1/4° global grid and the gaps are filled by interpolation (Reynolds et al., 2007).

Salinity data for the Mediterranean Sea are obtained from DIVA (data-interpolating variational analysis); this tool allows to interpolate in situ observations to obtain gridded climatologies (Brasseur et al., 1996).

https://doi.org/10.5194/gmd-2020-248
Preprint. Discussion started: 8 January 2021


Geoscientific Model Development Discussions

For the mixed layer depth, we use a global climatology computed from more than one million Argo profiles collected from 2000 to present (Holte et al., 2017); this climatology provides estimates of monthly mixed layer depth on a global 1° gridded map.

As reference dataset to evaluate the performances of the atmospheric components of the ENEA-REG system we use ERA5: this allows to test model's ability to reliably reproduce their parent data (Mooney et al., 2013) and because, unlike other observational data, this dataset provides information on both over land and ocean.

The observed river discharge of the Po river has been extracted from the series of measures at the Ponte Lagoscuro station from the RivDIS dataset (Vorosmarty et al. 1998)

4. Results

4.1 Evaluation of atmospheric models

The general ability of the atmospheric components of the ENEA-REG system to reproduce realistic spatio-temporal patterns of the most relevant physical variables is assessed by comparing model simulations with ERA5 during winter (DJF) and summer (JJA) seasons averaged over the reference period 1982-2013. In the present analysis, in addition to spatial patterns and anomalies maps, we also compute correlation patterns and domain-averaged bias to provide a measure of the model's skills.

Looking at the surface air temperature (**Figure 3**), consistent with ERA5 data, during winter both WRF and RegCM show a typical eastward gradient with temperature decreasing with increasing continentally, while during summer the models correctly reproduce the decreasing south-north gradient with colder areas localized over mountainous regions (i.e. Alps and Pyrenees). Looking at the anomalies, WRF shows a remarkable cold bias during DJF over northeastern Europe, with magnitudes larger than 4 °C. Such a cold bias over this region was already described in several studies and it mainly depends on the choice of WRF physical parameterizations (e.g. Moonet et al., 2013; Kotlarski et al., 2014; Katragkou et al., 2015). In a sensitivity study, where different physical parameterizations schemes were used to represent radiation, microphysics, convection, PBL and land surface, Mooney et al. (2013) reported that the simulated summer surface air temperature is mostly controlled by the selection of land surface model, while during winter the temperature shows some sensitivity to longwave radiation and very little sensitivity to other parameterizations. Despite, when setting up WRF, we were aware of both the need to carefully

https://doi.org/10.5194/gmd-2020-248
Preprint. Discussion started: 8 January 2021


Geoscientific Model Development Discussions

select parameterization combinations and the issues associated with some of the selected parameterizations, we chose the present settings as they well reproduce wind fields over the Mediterranean region, which is relevant when running WRF coupled with an ocean model. Besides, as demonstrated by Mooney et al. (2013), over such a large domain, no single combination of parameterizations yields optimal results. Unlike WRF, RegCM does not show any remarkable bias during winter and, in general, it shows a cold bias ranging between 1 and 2 °C over the whole Mediterranean region. The good spatial agreement found during DJF between the simulated surface air temperature and the reference data is confirmed by the high spatial correlation varying between 0.98 in case of WRF to 0.99 for RegCM, while the domain-averaged bias ranges from -1.3°C for WRF to -0.15°C for RegCM.

During summer, both WRF and RegCM show a similar bias pattern, with a warm bias extending from France to Eastern Europe and reaching magnitudes of up to 3 °C in case of RegCM. This result is consistent with Turuncoglu and Sannino (2017) who described a similar behaviour running RegCM both standalone and coupled to ROMS ocean model, with a temperature overestimation up to 2.0–2.5 °C during the summer season in central and eastern Europe. Overall, our regional models well reproduce the observed spatial pattern, being the spatial correlation larger than 0.99 for both WRF and RegCM. Considering the domain-averaged bias, during JJA the configuration using WRF shows a slightly lower warm bias (0.1 °C) compared to RegCM (0.14 °C).

Looking at precipitation, during winter both the ENEA-REG configurations have a good agreement with ERA5 data, namely the atmospheric components are able to reproduce the major precipitation maxima over the Alps, Balkans and western Norway with only a substantial local dry bias in the areas around the coastlines of eastern Mediterranean. In contrast, during summer, WRF and RegCM systematically simulate less precipitation over most of continental Europe, with RegCM showing the largest dry bias (**Figure 4**). Interestingly, considering WRF, these results are not consistent with Mooney et al. (2013), who reported a positive bias in mean daily precipitation over Europe during summer and related this wet bias to the land surface scheme used and partially to the microphysics scheme. However, Kotlarski et al. (2014) comparing three WRF experiments showed a different sensitivity, with two simulations overestimating mean summer precipitation and one underestimating it; they conclude that this result depends on the

https://doi.org/10.5194/gmd-2020-248
Preprint. Discussion started: 8 January 2021


Geoscientific Model Development Discussions

choice of different microphysics schemes. On the other side, Turuncoglu and Sannino (2017) found a similar bias pattern for RegCM during summer.

In general, the spatial performances of the ENEA-REG system are better when WRF is used as the atmospheric component: the spatial correlation ranges between 0.97 during DJF to 0.95 during JJA, while the configuration with RegCM exhibits a slightly lower pattern correlation (0.95 for DJF, 0.92 during JJA). Similarly, WRF has a smaller bias during summer (-0.42 vs -0.54 mm/day), while during winter RegCM shows slightly better performances (-0.24 mm/day) with respect to WRF (-0.27 mm/day); nevertheless, looking at **Figure 4** it should be noted that the better performances of RegCM during winter are mainly explained by compensation between dry and wet bias.

Despite the weak summer bias, the two atmospheric models well reproduce precipitation over the sea, enhancing the reliability of freshwater flux exchanged with the ocean component of the ENEA-REG system. Nevertheless, it should be noted that in the framework of coupled ocean-atmosphere models, rather than precipitation, the water budget, defined as evaporation–precipitation (E–P), plays a pivotal role in the dynamics of the ocean component. For this reason, in **Figure 5** we show both the simulated inter-annual variability and mean seasonal cycle of the area-averaged Mediterranean Sea precipitation, evaporation along with their difference (i.e. E-P). Looking at precipitation, WRF shows a systematic dry bias over sea with respect to ERA5, while RegCM is in good agreement with the reference value. The mean annual cycles suggest that WRF underestimates rainfall during cold months (from November to March), while RegCM well reproduces the observed seasonal cycle, with a weak overestimation between August and October. Overall, the two configurations of ENEA-REG system well reproduce the reference seasonal cycle, characterized by maximum values during fall and winter and minimum in summer (JJA).

The total precipitation over the Mediterranean Sea is 409±41 mm/yr using WRF as atmospheric component and 496±48 mm/yr in case of RegCM, while ERA5 predicts 469±50 mm/yr. In general, these estimates agree with previous studies: in particular, in a different experiment, where WRF was coupled with NEMO ocean model, Lebeaupin-Brossier et al. (2015) found a precipitation budgets of 482±53 mm/yr over the period 1989–2008, concluding that this value is in the upper part of the range given in the literature [290–510 mm/yr] (Mariotti et al. 2002; Pettenuzzo et al. 2010; Romanou et al. 2010; Criado-Aldeanueva et al. 2012). Similarly, in a

https://doi.org/10.5194/gmd-2020-248
Preprint. Discussion started: 8 January 2021


Geoscientific Model Development Discussions

regional climate system model developed over the Mediterranean Sea, where RegCM was coupled with ROMS ocean model, Turuncoglu and Sannino (2017) found a mean annual precipitation of 561 mm/yr during the temporal period 1988–2006; however, they also showed a large variability in the estimates depending on the land-sea mask used to process data. In a different configuration, where ALADIN climate model was coupled with NEMO ocean model, Sevault et al. (2014) found a precipitation of 510 mm/yr over the time period 1980-2012, while Sanchez-Gomez et al. (2011) compared 12 regional climate models finding a large spread among models with mean annual precipitation estimates ranging between 347 and 606 mm/yr with a mean value of 442±84 mm/yr.

Compared to ERA5, the evaporation is systematically overestimated by both RegCM and WRF during our study period, despite the year-to-year variability is well reproduced and the mismatch decreases with time (**Figure 5**); while in case of WRF this overestimation is mainly found between April-September, RegCM overpredicts the evaporation during all months. Nevertheless, the two configurations correctly reproduce the seasonal cycle, characterized by evaporation minimum in May and maxima during late summer and winter months, when the gradient between air–sea temperature is high and the wind speed is strong. The total evaporation over the Mediterranean Sea is 1299±30 mm/yr and 1405±38 for WRF and RegCM, respectively, while ERA5 has lower evaporation of 1198±59 mm/yr. Consistent with precipitation, our estimates well agree with previous studies: Lebeaupin-Brossier et al. (2015) using WRF coupled to NEMO found a total evaporation of 1442±45 mm/yr during the 1989–2008 period, while Turuncoglu and Sannino (2017) using RegCM coupled to ROMS reported a value of 1388 mm/yr during the 1988–2006 period. Sevault et al. (2014) estimated a mean annual evaporation of 1390 mm/yr, while Sanchez-Gomez et al. (2011) displayed a large variability among 12 regional climate models, with annual mean estimates ranging between 1066 mm/year and 1618 mm/year, this latter using RegCM offline forced by ERA40 data. The comparison with previous studies highlights a general tendency of RegCM to overestimate the evaporation over the Mediterranean sea, irrespective of the forcing data and parameterizations selected; this could be likely caused by an overestimation of wind speed (discussed later).

Interestingly, because of bias compensation WRF and RegCM show a similar E-P estimate (**Figure 5**); however, we found in both the configurations of the ENEA-REG system a remarkable bias in E-P, with values larger than 100 mm/year, which could significantly affect the

https://doi.org/10.5194/gmd-2020-248
Preprint. Discussion started: 8 January 2021


Geoscientific Model Development Discussions

ocean component. The monthly distribution of E–P shows, in both the ENEA-REG configurations, a similar monthly distribution with ERA5 dataset with a peak in the late summer caused by sparse precipitation and high evaporation. The total E-P estimated simulated using WRF is 890±43 mm/yr while with RegCM we obtain a mean annual estimate of 909±45 mm/yr; in contrast, ERA5 data has a lower E-P of 729±56 mm/yr.

In addition to freshwater flux, wind speed is also a key variable for ocean models as it controls the evaporation over the sea surface and affects the ocean circulation through the drag stress. **Figure 6** shows the near-surface wind speed as simulated by the ENEA-REG system and ERA5 reanalysis. The comparison with the observationally based dataset indicates that both WRF and RegCM overestimate the wind speed over land during the two analyzed seasons, while over sea the atmospheric models are able to correctly simulate the wind speed, especially over the Gulf of Lion and the Aegean sea, where the structure and magnitude of dominant Mistral and Etesian winds is well reproduced by WRF. In contrast, RegCM shows too weak Etesian during summer and a general positive bias over the whole Mediterranean basin during DJF. This overestimation by RegCM has a remarkable effect of deep water formation in the Levantine basin and affects the deep convection and the mixed layer depth simulated by the ocean model (discussed later); in addition, it is responsible for the large evaporative flux described in **Figure 5**.

It should also be noted that the large bias found over mountainous regions is clearly an artifact due to the spatial resolution differences, with ERA5 reanalysis reproducing lower wind speed than both WRF and RegCM because of its coarser resolution. In general, the two atmospheric models have comparable performances in reproducing the observed spatial pattern; we find a correlation of 0.98 for both models and seasons, except for RegCM during summer (0.97). In contrast, WRF has a lower bias (1 m/s for DJF and 0.87 m/s for JJA) than RegCM (1.4 m/s for DJF and 1.2 m/s for JJA). The higher agreement of WRF with ERA5 is a direct consequence of the spectral nudging of wind data above the PBL.

Besides to freshwater flux and wind components, the surface net heat flux is used to drive the ocean model of the ENEA-REG system (**Figure 1**); this variable represents the energy that the ocean surface receives from the atmosphere and is computed from net longwave, net shortwave, latent heat and sensible heat fluxes. Each component of the heat balance equation represents a way ocean can gain or loss heat from the atmosphere: the latent heat flux controls the heat loss by the ocean through evaporation, the sensible heat flux represents the heat loss by the ocean by

https://doi.org/10.5194/gmd-2020-248
Preprint. Discussion started: 8 January 2021


Geoscientific Model Development Discussions

399 conduction to the atmosphere, the net shortwave radiation is the energy the ocean gains from the
400 Sun less a small amount of energy loss because of surface albedo, while the net longwave
401 radiation is the difference between the radiant energy emitted by the ocean and radiant energy
402 received from the atmosphere.
403 In **Figure 7** we compare the simulated net energy flux with ERA5 data; overall, the two
404 atmospheric models are in good agreement with the reference dataset during the analyzed
405 seasons, albeit a complex bias pattern is evident over the Mediterranean sea with WRF and
406 RegCM showing an interesting bias of opposite sign during summer and winter. The models
407 show similar skills in reproducing the ERA5 spatial patterns, both having a correlation of 0.96
408 during DJF, while in JJA RegCM (0.97) is slightly better than WRF (0.96); similarly, RegCM
409 also exhibits the lowest bias during both DJF (-1.3 W/m^2 vs 7.8 W/m^2) and JJA (3.1 W/m^2 vs
410 10.3 W/m^2). Looking at the spatial bias in more details, WRF shows a systematic positive bias
411 over the land surface up to 10 W/m^2 during winter and 15-20 W/m^2 in summer, while RegCM
412 well matches ERA5 data in DJF with bias lower than 5 W/m^2 but with a systematic negative bias
413 over the land ranging between -10 W/m^2 and -15 W/m^2 during JJA.
414 To further extend the analysis, in **Figure 8** we compare the monthly climatology of energy flux
415 components averaged over the whole Mediterranean Sea with ERA5 data. The analysis of model
416 results suggests that the latent heat is systematically overestimated by RegCM during the whole
417 year, whereas WRF is in good agreement with ERA5 during cold seasons (between October and
418 March) and it overestimates the latent heat flux in the remaining months (**Figure 8a**). The annual
419 mean estimates are 103±2.4 W/m^2 from WRF and 112±2.9 W/m^2 from RegCM, with ERA5
420 showing a slightly smaller flux (95±4.7 W/m^2). This result confirms previous findings about
421 RegCM, namely the too intense wind speed leads to a large latent heat flux and hence to an
422 overproduction of evaporative flux. In addition, our results are consistent with previous studies;
423 in particular, Turuncoglu and Sannino (2017) reported a value of 110.52 W/m^2 from RegCM
424 coupled to ROMS, whilst Sanchez-Gomez et al. (2011) showed a value of 128±5 W/m^2; in this
425 latter study, RegCM showed the largest overestimation of latent heat flux among 12 regional
426 climate models.
427 The sensible heat flux shows a similar behavior to that observed for the latent heat, namely
428 RegCM systematically overestimates this variable during the whole year, whilst WRF is closer to
429 the reference data (**Figure 8b**). The annual mean estimates are 12.9±1.2 W/m^2 from WRF,

https://doi.org/10.5194/gmd-2020-248
Preprint. Discussion started: 8 January 2021


Geoscientific Model Development Discussions

17.6±1.2 W/m^2 from RegCM, while ERA5 has a slighter lower flux of 11.7±1.1 W/m^2. Interestingly, using RegCM coupled to ROMS, Turuncoglu and Sannino (2017) found a smaller sensible heat flux of 9.85 W/m^2, while Sanchez-Gomez et al. (2011) running RegCM offline reported a value closer to our estimate (22±2 W/m^2); as the sensible heat strictly depends on the gradient between SST and air temperature the lower value of Turuncoglu and Sannino (2017) could be explained by a large discrepancy between the SSTs simulated by the MITgcm and the ROMS ocean models.

The mean annual cycle of net shortwave radiation is well simulated by the atmospheric models, with WRF showing a perfect match compared to ERA5, while RegCM underestimates the summer peak of about 25 W/m^2 and slightly overestimates the amount of radiation received by the ocean from January to April (**Figure 8c**). The mean annual estimates are 199±1.2 W/m^2 form WRF, 201±1.2 W/m^2 form RegCM and 198±1.1 W/m^2 form ERA5; for both the ENEA-REG configurations, these estimates are in agreement with other studies (Sanchez-Gomez et al., 2011; Turuncoglu and Sannino, 2017).

The comparison of simulated net longwave radiation with ERA5 data indicates that RegCM underestimates the thermal radiation during the whole year, while WRF is in fair agreement between March and October and overestimates the longwave radiation in the other months (**Figure 8d**). In addition, the amplitude of seasonal variation is well captured by RegCM; in contrast, WRF shows a stronger month-to-month variability. The mean annual net lonwave radiation simulated by RegCM is -77.6±1.2 W/m^2, while WRF predicts -85.6±3.9 W/m^2 which is very close to ERA5 dataset (-84.8±1.2 W/m^2).

4.2 Evaluation of ocean model

4.2.1. Surface processes

The correct representation of physical processes taking place at the air-sea interface is crucial for the success of a coupled climate simulation. A first evaluation of the goodness with which these processes are simulated is given by the analysis of the ocean surface variables like Sea Surface Temperature (SST) and Sea Surface Salinity (SSS).

Figure 9 shows the comparison of simulated SST with OISST reference data. We recall that SST, in a coupled simulation, is actually the same variable for ocean and atmosphere components (where grids overlap), and guides the thermal exchange providing an active

https://doi.org/10.5194/gmd-2020-248
Preprint. Discussion started: 8 January 2021


Geoscientific Model Development Discussions

feedback among the two components: the higher is the difference among SST and atmosphere temperature, the larger will be the heat exchange at the interface that tends to lower such difference. Looking at **Figure 9**, the coupled model well reproduces the OISST spatial pattern with an agreement larger than 0.99 for both the configurations and seasons.WRF-MITgcm shows moderate biases during winter (-0.24°C) and summer (0.23°C) while RegCM-MITgcm has a widespread negative bias in winter (-0.9°C) and a positive bias in summer (0.25°C), with marked spatial patterns in the eastern part of the Levantine Sea during winter and in the Sardinian Sea during summer; it should be noted that the spatial average over the entire basin reduces the bias within one degree, although the differences can be locally much more relevant, especially in the RegCM-MITgcm configuration.

In spite of some large local bias, the RegCM-MITgcm well reproduces the observed interannual variability, although it has a too marked year-to-year variability; in contrast, WRF-MITgcm well captures the observed SST monthly anomalies (**Figure 10a**). Moreover, the WRF-MITgcm SST seasonal cycle closely follows the reference dataset, while RegCM-MITgcm shows a considerable SST underestimation between December and April and a slight overestimation in the summer months (**Figure 10b**). Compared to similar modeling experiments, we note that an overall cold bias is not unusual in coupled simulations of the Mediterranean Sea and the magnitude of the biases obtained in the present study is comparable to the literature (Sevault et al., 2014, Turuncoglu and Sannino, 2017, Reale et al.2020). In particular, the seasonal spatial patterns in winter and summer closely resemble those shown in Turuncoglu and Sannino (2017), although they used the ROMS model to simulate the Mediterranean Sea. More recently, Reale et al. (2020) obtained a reduced cold bias with respect to both the available literature and the present experiment performed with RegCM-MITgcm; however a direct comparison is not straightforward as their simulation period was limited to the years 1994-2006. Conversely, considering WRF-MITgcm, our results are slightly better than similar simulations, being the bias well below 0.3°C and no remarkable local bias are evident during the analyzed seasons.

Considering the SSS, compared to the reference data, both the simulations show very similar spatial patterns and biases (**Figure 11**); we found the ocean model, in both its configurations, saltier than the reference dataset, especially in the Adriatic Sea during summer. This is due to the fact that the Adriatic Sea is a dilution basin, mainly because of the important freshwater supply provided by rivers. In both the simulations the freshwater input from river runoff is heavily

https://doi.org/10.5194/gmd-2020-248
Preprint. Discussion started: 8 January 2021


Geoscientific Model Development Discussions

underestimated by the interactive river routing model (**Figure 12**); this underestimation is more evident in RegCM as a consequence of the larger drier precipitation bias found over land (**Figure 4**), resulting in a lower river baseline with respect to WRF (**Figure 12**).

Looking at the monthly SSS anomalies (**Figure 13a**) we found a similar temporal variability compared to the reference data. Besides, the two configurations of the coupled model fairly agree, although occasionally they are very different, as it happens in 1996, when WRF has an remarkable drop in SSS due to the minimum in the freshwater flux (**Figure 5**) caused by exceptional precipitation and river runoff during that year; interestingly, such a drop is also evident in other observational datasets (Sevault et al., 2014).

Unlike the monthly SSS anomalies, the seasonal cycle of SSS for the two simulations is very similar during all the months (**Figure 13b**), coherently with the freshwater flux seasonal cycle, although both E and P over sea are more intense in RegCM than in WRF (**Figure 5**). Compared to other studies, the mean bias of both WRF-MITgcm and RegCM-MITgcm is lower than that of similar simulations for the Mediterranean Sea as it does not exceed 0.1 g/km on a basin mean (e.g. Sevault et al., 2014, Turuncoglu and Sannino, 2017).

4.2.2 Sea surface height and circulation

The Strait of Gibraltar is the only connection between the Mediterranean basin and the Atlantic Ocean. In general, the two-way exchange at the strait is constituted by an upper inflow of Atlantic water and a lower outflow of relatively colder and saltier Mediterranean water. However, the semidiurnal tidal effect is strong enough to reverse the direction of the flows during part of the tidal cycle. As this exchange represents the main driver of the circulation in the basin, the estimation of its value has been faced for decades.

The inflow transport derived from the two coupled simulations is about 1 Sv (**Table 2**); similarly, the models predict a net transport of 0.06 Sv. Unfortunately, the estimate of the transport obtained from the direct measurements of velocities is affected by the limited number of moorings used that cannot resolve the structure of the entire section. Therefore, some numerical models have also been used to reproduce and quantify the two way-exchange . Estimates of mean inflow range from about 0.72 Sv of Bryden et al. (1994) to 1.68 Sv of Bethoux (1979). Sannino et al. (2009) computed an inflow of 1.03 Sv using a three-dimensional

https://doi.org/10.5194/gmd-2020-248
Preprint. Discussion started: 8 January 2021


Geoscientific Model Development Discussions

numerical model characterized by a very high resolution in the strait. Similarly, the long-term net transport that balances the excess of evaporation over precipitation and river runoff in the Mediterranean has a value of about 0.05 Sv (Bryden et al. 1994; Sannino et al., 2009); noteworthy, our results well agree with these estimates (**Table 2**).

The Sicily strait connects the western and the eastern Mediterranean basins. The Modified Atlantic Water (MAW) flows eastward in the upper layer and the Levantine Intermediate Water (LIW) below it, in the opposite direction. Transports computed for this channel in the two simulations are very close, with an eastward value of about 1.3 Sv and a net of a few hundredth of Sv. These results are in agreement with the estimate of 1.1 Sv obtained in the experimental work of Astraldi et al. (1999) and with the numerical model estimates ranging from 0.7Sv to 1.2 Sv (Fernandez et al. 2005, Zavatarelli & Mellor, 1995, Béranger et al. 2005).

The mean annual current velocity at 30 m depth and the mean annual Sea Surface Height (SSH) are analyzed in **Figure 14** for WRF-MITgcm (a) and RegCM-MITgcm (b), respectively. The two simulations depict a similar mean annual circulation, both at the surface (i.e SSH) and at the intermediate level (i.e. velocities), with similar large-scale features.

The Atlantic Water (AW) circulation picture is in good agreement with those described by Millot and Taupier-Letage (2005) and Pinardi et al. (2013), the first being mainly based on both in situ and remotely sensed datasets, the latter resulting from a reanalysis performed with a model having an horizontal resolution of 1/16° x 1/16°. In particular, Atlantic surface waters enter at Gibraltar, are trapped into gyres in the Alboran Sea and then exit, dividing into two branches: one sticking to the North-African coast, forming the Algerian current and the other in the direction of the Balearic Islands. This latter detaches from the coast and flows south of Ibiza Island generating an intense jet flowing eastward. This current receives the contribution of the Southern edge of the Lion cyclonic gyre after the Balearic Sea and generates the Southern Sardinian Current flowing along the west coast of Sardinia and merging with the Algerian current. The Southern Sardinian Current branches in three parts (Béranger et al., 2004; Pinardi et al., 2006): the southernmost branch produces the Sicily Strait Tunisian current, the central one forms the Atlantic Ionian Stream (Robinson et al., 1999; Onken et al., 2003; Lermusiaux and Robinson, 2001) and the northernmost one enters in the Tyrrhenian Sea giving rise to the South-Western Tyrrhenian gyre. Finally, the Atlantic waters penetrate into the eastern basin through the Sicily Strait. Noticeably, all these structures are very well defined in both the configurations of

https://doi.org/10.5194/gmd-2020-248
Preprint. Discussion started: 8 January 2021


Geoscientific Model Development Discussions

the regional Earth system model (**Figure 14**). In addition, in the western Mediterranean basin, the two model's versions show a wide cyclonic gyre, including the liguro-provencal current in the Gulf of Lions.

The mean circulation in the Eastern basin is characterized by several features common to both simulations. It is possible to appreciate how the surface water penetrates into the Adriatic Sea with a cyclonic circulation, and it is possible to notice the presence of a counterclockwise circulation in the Aegean Sea in both simulations; the WRF-based configuration is characterized by a more intense eastward jet crossing the Eastern basin (**Figure 14**).

Also, the simulations reproduce quite clearly the places where deep water formation takes place: the three cyclonic gyres located in the Gulf of Lyon, southern Adriatic Sea and in the Levantine Sea. These cyclonic gyres concur with negative SSH values, which highlight the sinking of surface waters.

4.2.3 Heat and salt contents

Mean annual temperature and salinity averaged over the entire Mediterranean basin and the Western and Eastern sub-basins are shown in **Table 3**; here we present estimates from the DIVA data, while for the two simulations we show the anomalies with respect to the reference data. The average content of heat and salt has been computed over different vertical layers: the entire column, the surface layer (0 -150m) corresponding approximately to the Atlantic Water, the intermediate layer (150-600m) representing mainly the Levantine Intermediate Water, and the deep layer (600-3500m) containing the Eastern and Western Mediterranean Deep Waters.

The average temperature of the whole water column, for each sub-basin, is in good agreement with observations in both coupled runs, being the difference between modeled values and observations not exceeding 0.2°C. Major discrepancies are concentrated in the upper layer of the Eastern basin, where both models result colder than observation, with WRF-MITgcm showing an underestimation of 0.45°C, while RegCM-MITgcm has a bias exceeding 1°C. Such discrepancy reduces within the intermediate layer, while there is a slight overestimation in the deep layer, that quite compensates for the error in the uppermost layers, when the total average is computed. In the western basin the two models remain much closer to the observations, although RegCM-MITgcm shows a systematic cold bias and WRF-MITgcm a systematic warm bias; however, WRF is always closer to observations than RegCM. Notwithstanding the bias, we point out that

https://doi.org/10.5194/gmd-2020-248
Preprint. Discussion started: 8 January 2021


Geoscientific Model Development Discussions

the mean values of the temperature within the different layers are compatible with those obtained in analogous simulations, and are within the ensemble spread computed from the series of Med-Cordex simulations analyzed by Llasses et al. (2018).

Figure 15 shows the time series of mean annual temperature anomalies computed over the 1982-2013 period for the surface and intermediate layers in the whole basin and in the Western and Eastern sub-basins. Generally, the interannual variability of the whole basin is well captured by the two simulations in both the surface layer and in the intermediate level. WRF-MITgcm is remarkably close to observations between 0-150 m, while in the intermediate layer small differences occur at the beginning of the simulations. The RegCM -MITgcm simulation shows a slightly different behaviour with respect to observed data especially after the year 2006, when the intensity of the positive anomalies is underestimated in both layers, although the year-to-year variability is well reproduced. Altough the same general considerations hold for each of the two sub-basins, we observe that WRF-MITgcm remarkably well captures the surface positive anomaly in 1990 in the western basin, as well as the sequence of negative anomalies in the eastern basin (1983,1987, and 1993). In the intermediate layer, the sudden drop of temperature during 1993 is the signature of the Eastern Mediterranean Transient (EMT) phenomenon (discussed in paragraph **4.2.4**).

The mean annual salinity averaged over the whole column (**Table 3**) is slightly overestimated in both simulations (0.06 psu) mainly due to an overestimate of the salt content in the eastern sub-basin. In the Eastern basin the maximum of salinity is correctly found in the intermediate layer (150-600m), in correspondence of the LIW, although the RegCM-MITgcm simulation shows a too slight decrease of the salinity from the intermediate to the deep layer. Such behaviour is consistent with the higher values reached by the Mixed Layer Depth (MLD) in the same area with respect to the MLD of the WRF-MITgcm simulation (discussed in paragraph **4.2.4**).

Similarly, in the western basin saltier intermediate water is clearly identified in the WRF run with respect to RegCM, due to the combined effect of the advection of a saltier LIW and a less intense deep convection, that in the western basin is mostly concentrated in the Gulf of Lion area. The comparison of the MLD in the Gulf of Lion area (see paragraph **4.2.4**) supports this hypothesis.

Figure 16 shows the time series of mean annual temperature anomalies computed over the 1982-2013 period for the surface and intermediate layers in the whole basin and in the Western and

https://doi.org/10.5194/gmd-2020-248
Preprint. Discussion started: 8 January 2021


Geoscientific Model Development Discussions

Eastern sub-basins. While the entire basin variability is generally well reproduced, the behaviour of models in the two sub-basins deserves some comment. In particular, in the western basin the RegCM-MITgcm simulation fails in reproducing the drop in salinity of the uppermost layer during the years 1990-1995. This is probably due to a too low freshwater flux in the RegCM-MITgcm simulations in those years, confirmed by high values of the MLD. On the other hand, in the eastern basin the WRF-MITgcm shows a freshwater anomaly in the 0-150m layer during the years 1995-1997 that is not detectable in the reference data. However, it should be noted that the same anomaly has also been observed in the SSS time series and is caused by exceptional precipitation and river runoff as already reported by Sevault et al. (2014). Anyhow, such a drop seems to affect mainly SSS and the surface layer, while it is scarcely transferred below 200 m. In the intermediate layer both simulations show a steady increase in the salinity anomaly. RegCM-MITgcm has almost a linear increase throughout the entire simulation period, due to the excess of surface salinity and anomalous deep convection in the Levantine Sea, while WRF-MITgcm is quite stable during the first half of the simulations and then shows a steep linear increase from 2000 onward.

4.2.4 Deep water formation

The formation of intermediate and deep waters due to sinking of dense water is one of the fundamental processes taking place in the Mediterranean Sea, in both the Eastern and Western sub-basins. Typical regions interested by this process are the Gulf of Lion, the South Adriatic, the Cretan Sea and the Rhode Gyre. Such a process, mainly driven by the strong air-sea interactions, takes place during the winter season, and is more effective during February. The most active region for deep water formation is the Gulf of Lion, while intermediate and deep waters are usually formed in the Adriatic and Levantine Sea, respectively.

The MLD is related to thermodynamic properties of seawater and is a pivotal variable helping in the identification of deep-water formation events. High MLD values are related to strong air-sea processes taking place at the surface or to preexisting stratification of the whole water column.

Figure 17 compares the simulated monthly maximum MLD computed over most important convective areas, i.e. the Levantine Sea, the Gulf of Lion, and the Adriatic Sea. Overall, RegCM-MITgcm shows a more intense convection activity with respect to WRF-MITgcm, reaching the deepest levels in all the analyzed regions. Looking at the Levantine region (**Figure 17a**), during

https://doi.org/10.5194/gmd-2020-248
Preprint. Discussion started: 8 January 2021


Geoscientific Model Development Discussions

almost the entire simulation, the MLD simulated by RegCM-MITgcm exceeds 1000m depth, while in case of WRF-MITgcm, the MLD is more variable in time. The latter is often less than 1000m and reaches the entire water depth during a few events, which are well known and documented also in observations (Lascaratos et al. 1999; Malanotte et al., 1999; Roether et al., 2007). These events (1983,1987 and 1989), corresponding to intense atmospheric fluxes, have favoured the preconditioning of the eastern basin leading to the well-known phenomenon of the EMT. Therefore, we can conclude that the LIW formation is better reproduced in the simulation that has WRF as an atmospheric component.

Similarly, several MLD observation-based estimates are available in the Gulf of Lion for the period covered by our simulations (e.g. Martens and Schott 1998; Schroeder et al., 2008; Somot et al., 2016). Compared to these estimates, we observe that WRF-MITgcm simulation closely follows the timing of deep water formation in the Western Mediterranean, in particular the deep convection events of 1987 and 2005, with the exception of 1991 and 1992, identified by Somot et al. (2016) as years of intense mixing; in contrast, RegCM-MITgcm systematically presents a deeper MLD (**Figure 17b**).

In addition to the temporal evolution of MLD, in **Figure 18** we compare the mean spatial pattern of the MLD with ARGO data (Holte et al., 2017). Results suggest that the RegCM-MITgcm simulation not only reaches higher depths but also the downwelling regions are much more extended compared to both ARGO data and WRF-MITgcm simulation. This is particularly evident in the Levantine basin and, to a lesser extent, in the Western Mediterranean where the downwelling area extends from the Gulf of Lion to the Ligurian Sea.

The steady-state picture of the Mediterranean thermohaline circulation, in which the Eastern Mediterranean Deep Water (EMDW) is only of Adriatic origin, has been called into question by the discovery of the EMT. As described by many authors, there is observational evidence that during the '90s the main source of EMDW migrated to the Aegean Sea (Lascaratos et al., 1993; Malanotte et al., 1999; Wu et al., 2000; Roether et al., 2007; Beuvier et al., 2010). The common understanding is that the EMT has been the effect of many concurrent causes that make this process difficult to be simulated: the large heat loss from surface in the Levantine, the shifting from cyclonic to anticyclonic circulation in the Ionian that prevents the entering of freshwater in the Levantine basin, and the lower than usual freshwater flux from the Black Sea. Waters formed in the Aegean are warmer and saltier than that of the Eastern Mediterranean at the same levels,

https://doi.org/10.5194/gmd-2020-248
Preprint. Discussion started: 8 January 2021


Geoscientific Model Development Discussions

and they are found at intermediate levels between LIW and EMWD of Adriatic origin. During the EMT period, instead, bottom levels were filled with newly formed waters of Aegean origin, while the less dense Adriatic waters were uplifted (Roether et al., 2007). All the studies agree on a massive dense-water formation in the Aegean Sea during the period 1987-1994 (e.g. Theocharis et al., 2002); as described by Theocharis et al. (1999), during the period 1986-1987, the Cretan Sea was characterized by a weak stratification. In the following years, water with densities higher than 29.2 was found at progressively upper layers in the Cretan Sea, with a significant formation rate in particular during 1989, due to an intrusion of deep waters from the central Aegean through the Myconos-Ikaria strait (Vervatis et al., 2013). Starting from 1989 dense water outflowed from the Cretan Arcs and was found in the Eastern Mediterranean Sea at levels between 700 and 1600 m. Then, dense water formation in the Cretan Sea increased during 1991 and 1992, the new water reached the upper layer of the Cretan basin, and the entire basin was filled with young water with density up to 29.3.

This phenomenon is remarkably well reproduced by the WRF-MITgcm simulation, both considering the timing of events and the density and volumes of newly formed waters, as shown in **Figure 19.** Here is depicted the volumes occupied by water with density higher than 29.2 kg/m3 and 29.3 kg/m3 in the Cretan Sea are; it can be seen that the period between 1983 and 1993 is characterized by an increase of the volume with three most significant peaks in 1984, 1989, and the highest in 1993, in both the simulations. Comparing with Sevault et al. (2014), the WRF-MITgcm has very similar behaviour with respect to both the timing of the events and the volumes formed, although they showed the whole Aegean Sea rather than the only Cretan Sea. In the 29.3 time series the event of 1993 is remarkably high, as expected, being this event the clear signature of the EMT. In contrast, RegCM-MITgcm is characterized by a more intense dense water formation, with the 29.2 water almost filling the Cretan basin during the whole simulation, while the 29.3 water almost fills the Cretan Sea in 1993, according to the EMT event. In the second part of the simulation, the volume of water filled with the densest water in the RegcM-MITgcm equals the volume occupied by the lower density water of WRF-MITgcm. Such an intense production of dense water in the Aegean Sea probably also affects the deep convection processes in the nearby Levantine Sea.

https://doi.org/10.5194/gmd-2020-248
Preprint. Discussion started: 8 January 2021


Geoscientific Model Development Discussions

5. Summary and conclusions

We presented a newly designed regional Earth system model used to study the climate variability over the Euro-Mediterranean region. The performances of individual model components were evaluated comparing results from the simulations with a wide range of observation-based datasets.

Unlike other existing coupled atmosphere–ocean models, our system is made up of two interchangeable atmospheric components (i.e. RegCM and WRF), offering thus the capability to select the regional atmospheric model to be used. For each atmospheric configuration, we performed a hindcast simulation over the period 1980-2013 using ERA-INTERIM reanalysis as lateral boundary conditions.

Overall, results indicate that both RegCM and WRF correctly reproduce both large-scale and local features of the Euro-Mediterranean climate, although some remarkable biases are relevant for some variables. In particular, while WRF shows a significant cold bias during winter over North-Eastern bound of the domain, RegCM systematically overestimates the wind speed over the Mediterranean Sea.

Similarly, the ocean component correctly reproduces the analyzed surface ocean properties, (along with their interannual variability) as well as the observed circulation in both the configurations of the coupled model. Anyhow, results also point out remarkable better performances when WRF is used to drive the ocean component of the coupled model; in fact, because of the systematic overestimation of wind speed by RegCM, the ocean model has a cold bias in SSTs during winter months and simulates a too deep mixed layer depth. This outcome is mainly evident for the EMT, for which we showed that WRF-MITgcm is able to reproduce the timing and the main characteristics of this event.

However, one could question that the overall better performances of WRF-MITgcm with respect to RegCM-MITgcm could be attributable to the spectral nudging. This method allows the passing of the driving model information not only onto the lateral boundaries but also into the interior of the regional model domain (Waldron et al.1996; Heikkilä et al., 2011); this is achieved by relaxing the model state towards the driving large-scale fields by adding a non-physical term to the model equation (Omrani et al., 2015). Clearly, the spectral nudging allows a stronger control by the driving forcing and thus a greater consistency between the regional model and large-scale climate coming from the driving model. Nowadays, there is still some controversy on

https://doi.org/10.5194/gmd-2020-248
Preprint. Discussion started: 8 January 2021


Geoscientific Model Development Discussions

the use of indiscriminate nudging in regional climate models (e.g. Omrani et al., 2015). Some studies agree that nudging does not allow the regional model to deviate much from the driving fields limiting the internal physics of the regional climate model (e.g. Sevault et al. 2014; Giorgi 2019). Considering the atmosphere-ocean coupling, Sevault et al. (2014) conclude that the use of spectral nudging strongly constrains the synoptic chronology of the atmospheric flow and thus the chronology of the air-sea fluxes and of the ocean response; they also found that this facilitates day-to-day and interannual evaluation with respect to observations, but nudging also limits the internal variability of the atmospheric component of the coupled model. Conversely, in a different study on extreme events in the Mediterranean Sea performed with a coupled atmosphere-ocean model, Lebeaupin-Brossier et al. (2015) found that nudging does not inhibit small scale processes and thus potential air–sea feedbacks are still simulated. This result is consistent with Omrani et al. (2015) who suggested that the spectral nudging technique does not affect the small-scale fields since only the large scales are relaxed.

Anyhow, to evaluate the sensitivity of the modeled surface variables to nudging, we performed the same simulation with WRF-MITgcm without nudging. Overall, results indicate that without nudging WRF-MITgcm has poorer performances and in general is in agreement with RegCM-MITgcm. For instance, considering the 2-m temperature over the Mediterranean sea, during DJF the bias with nudging is -0.19°C, while without nudging becomes -0.6°C, closer to RegCM (-0.96°C); similarly, during JJA the WRF bias increases significantly from 0.05 °C (with nudging) to 0.95°C (without nudging), while RegCM has a bias of -0.76°C. Likewise, the performances of the ocean model are strictly affected by the poorer performances of WRF without nudging: looking at SST the bias during winter is doubled (-0.21°C vs -0.54°C) but still lower than RegCM (-0.95°C), while during summer the performances of WRF-MITgcm without nudging (0.8°C) are even worse than RegCM-MITgcm (0.27°C), so much poorer that the same configuration using nudging (0.26°C).

This analysis reveals that spectral nudging helps to keep the large scale circulation of the regional model in phase with the driving model; however, we remark that nudging does not avoid the model to develop large local bias related to poor representation of some processes; this result is particularly clear for the cold bias during winter over North-Eastern bound of the domain (**Figure 3**).

https://doi.org/10.5194/gmd-2020-248
Preprint. Discussion started: 8 January 2021


Geoscientific Model Development Discussions

Notwithstanding the better performances, nudging has also to be used with caution: strong inconsistencies between regional model and driving large-scale fields may lead to unrealistic compensations within the model, for example, anomalous heat fluxes compensating for temperature biases (Brune and Baehr, 2020).

We conclude that in the context of coupled atmosphere-ocean models, the correct representation of surface winds is crucial to simulate ocean-atmosphere interactions correctly. In details, we noted that poor representation of winds by RegCM led to significant deviations from observations within the ocean model. This result is consistent with the poorer performances of RegCM-MITgcm that mainly depend on the large bias in surface wind speed introduced with RegCM. In this regard, as already discussed by Omrani et al. (2015), the wind above the PBL is a key variable to nudge to simulate surface temperature, wind, and rainfall correctly. As wind determines the transport of all conserved quantities like heat and moisture, their correct representation has a relevant impact on several other quantities.

Finally, the comparison with offline results (not shown) suggests that atmosphere-ocean coupling over the Mediterranean region remarkably changes the surface climate over the sea but, over continental Europe, the climate is poorly constrained by the coupling. This is because the large-scale systems mainly dominate the climate over central Europe originated in the Atlantic Ocean, as already discussed in other studies (e.g. Somot et al., 2008; Artale et al. 2010; Turuncoglu and Sannino, 2017). Nevertheless, as highlighted by Lebeaupin-Brossier et al. (2015), differences in SST between offline and coupled simulations directly affect the local evaporation and precipitation as well as the occurrences of extreme events.

Notwithstanding the low sensitivity of atmospheric components in the Mex-CORDEX region, coupled models remain useful tools to predict future climate over the Mediterranean area (Artale et al., 2010), which is widely recognized as climate change hot spot (e.g. Giorgi, 2006; Tuel and Eltahir, 2020).

Code availability

The source code of the RegESM driver is distributed through the public code repository hosted by GitHub (https://github.com/uturuncoglu/RegESM, last access: 24 December 2020). The version that is used in this study is permanently archived on Zenodo and accessible under the digital object identifier https://doi.org/10.5281/zenodo.4386712. The user guide and detailed

https://doi.org/10.5194/gmd-2020-248
Preprint. Discussion started: 8 January 2021


Geoscientific Model Development Discussions

information about the modeling system and how to compile it are also distributed along with the source code in the same code repository.

The standard version of WRF model is publicly available online at https://github.com/NCAR/WRFV3/releases/tag/V3.8.1 (last access: 24 December 2020) but the customized version that allow to couple with RegESM modeling system is permanently archived on Zenodo and accessible under the digital object identifier https://doi.org/10.5281/zenodo.4392230. The MITgcm model can be freely downloaded from its web page (http://mitgcm.org/source-code/ (last access: 24 December 2020) but the substantially modified version to allow coupling with RegESM modeling system can be accessible at https://github.com/uturuncoglu/MITgcm and it is permanently archived on Zenodo and accessible under the digital object identifier https://doi.org/10.5281/zenodo.4392260. The RegCM model can be downloaded from public GitHub repository (https://github.com/ictp-esp/RegCM, last access: 24 December 2020), while the HD model is available at https://wiki.coast.hzg.de/display/HYD/The+HD+Model (last access: 24 December 2020) but slightly customized version that enables coupling with RegESM modeling system can be accessed from the public GitHub repository (https://github.com/uturuncoglu/HD) and it is permanently archived on Zenodo and accessible under the digital object identifier https://doi.org/10.5281/zenodo.4390527. For each model, the coupling support is provided contacting the authors (alessandro.anav@enea.it; turuncu@ucar.edu; gianmaria.sannino@enea.it).

The initial and boundary meteorological conditions, provided by the European Centre for Medium-Range Weather Forecast (ECMWF), can be freely downloaded from the ECMWF web page (https://apps.ecmwf.int/datasets/data/) after registration.

The LEVITUS94 monthly climatology for temperature and salinity is available at the web page https://iridl.ldeo.columbia.edu/SOURCES/.LEVITUS94/.MONTHLY/ (last access: 24 December 2020). The Mediterranean and Black Sea database of temperature and salinity (MEDATLAS/2002) is available at http://www.ifremer.fr/medar/.

Author contributions

UT wrote the RegESM driver, while all the authors worked on the coding tasks to couple the model components through RegESM. AA and MS performed the simulations. All authors discussed the results and contributed to the writing of the article.

Competing interests

The authors declare that they have no conflict of interest.

Acknowledgements

The computing resources and the related technical support used for this work have been provided by CRESCO/ENEA-GRID High Performance Computing infrastructure and its staff

https://doi.org/10.5194/gmd-2020-248
Preprint. Discussion started: 8 January 2021


Geoscientific Model Development Discussions

(http://www.cresco.enea.it). CRESCO/ENEAGRID High Performance Computing infrastructure is funded by ENEA, the Italian National Agency for New Technologies, Energy and Sustainable Economic Development and by National and European research programs".

Financial support

This research has been supported by the SOCLIMACT project ("DownScaling CLImate imPACTs and decarbonisation pathways in EU islands, and enhancing socioeconomic and non-market evaluation of Climate Change for Europe, for 2050 and beyond"). UT is supported by the National Center for Atmospheric Research, which is a major facility sponsored by the National Science Foundation under Cooperative Agreement 1852977.

References

Adcroft, A., Hill, C., and Marshall, J.: Representation of topography by shaved cells in a height coordinate ocean model, Monthly Weather Review, 125, 2293-2315, 1997.

Adcroft, A., and Campin, J.-M.: Rescaled height coordinates for accurate representation of free-surface flows in ocean circulation models, Ocean Modelling, 7, 269-284, 2004.

Artale, V., Calmanti, S., Carillo, A., Dell'Aquila, A., Herrmann, M., Pisacane, G., Ruti, P. M., Sannino, G., Struglia, M. V., and Giorgi, F.: An atmosphere–ocean regional climate model for the Mediterranean area: assessment of a present climate simulation, Climate Dynamics, 35, 721-740, 2010.

Astraldi, M., Balopoulos, S., Candela, J., Font, J., Gacic, M., Gasparini, G., Manca, B., Theocharis, A., and Tintoré, J.: The role of straits and channels in understanding the characteristics of Mediterranean circulation, Progress in Oceanography, 44, 65-108, 1999.

Béranger, K., Mortier, L., Gasparini, G.-P., Gervasio, L., Astraldi, M., and Crépon, M.: The dynamics of the Sicily Strait: a comprehensive study from observations and models, Deep Sea Research Part II: Topical Studies in Oceanography, 51, 411-440, 2004.

Béranger, K., Mortier, L., and Crépon, M.: Seasonal variability of water transport through the Straits of Gibraltar, Sicily and Corsica, derived from a high-resolution model of the Mediterranean circulation, Progress in Oceanography, 66, 341-364, 2005.

Bethoux, J.: Budgets of the Mediterranean Sea. Their depenqance on the local climate and on the characteristics of the Atlantic waters, Oceanol. Acta, 2, 157-163, 1979.

Beuvier, J., Sevault, F., Herrmann, M., Kontoyiannis, H., Ludwig, W., Rixen, M., Stanev, E., Béranger, K., and Somot, S.: Modeling the Mediterranean Sea interannual variability during 1961–2000: focus on the Eastern Mediterranean Transient, Journal of Geophysical Research: Oceans, 115, 2010.

https://doi.org/10.5194/gmd-2020-248
Preprint. Discussion started: 8 January 2021

872 Brasseur, P., Beckers, J.-M., Brankart, J.-M., and Schoenauen, R.: Seasonal temperature and
873 salinity fields in the Mediterranean Sea: Climatological analyses of a historical data set, Deep
874 Sea Res. Part I, 43, 159– 192, 1996.

875 Breitkreuz, C., Paul, A., Kurahashi-Nakamura, T., Losch, M., and Schulz, M.: A dynamical
876 reconstruction of the global monthly mean oxygen isotopic composition of seawater, Journal of
877 Geophysical Research: Oceans, 123, 7206-7219, 2018.

878 Brossier, C. L., Bastin, S., Béranger, K., and Drobinski, P.: Regional mesoscale air–sea coupling
879 impacts and extreme meteorological events role on the Mediterranean Sea water budget, Climate
880 dynamics, 44, 1029-1051, 2015.

881 Brune, S., and Baehr, J.: Preserving the coupled atmosphere–ocean feedback in initializations of
882 decadal climate predictions, Wiley Interdisciplinary Reviews: Climate Change, 11, e637, 2020.

883 Bryden, H. L., Candela, J., and Kinder, T. H.: Exchange through the Strait of Gibraltar, Progress
884 in Oceanography, 33, 201-248, 1994.

885 Criado-Aldeanueva, F., Soto-Navarro, F. J., and García-Lafuente, J.: Seasonal and interannual
886 variability of surface heat and freshwater fluxes in the Mediterranean Sea: budgets and exchange
887 through the Strait of Gibraltar, International Journal of Climatology, 32, 286-302, 2012.

888 Darmaraki, S., Somot, S., Sevault, F., Nabat, P., Narvaez, W. D. C., Cavicchia, L., Djurdjevic,
889 V., Li, L., Sannino, G., and Sein, D. V.: Future evolution of marine heatwaves in the
890 Mediterranean Sea, Climate Dynamics, 53, 1371-1392, 2019.

891 Dee, D. P., Uppala, S. M., Simmons, A., Berrisford, P., Poli, P., Kobayashi, S., Andrae, U.,
892 Balmaseda, M., Balsamo, G., and Bauer, d. P.: The ERA-Interim reanalysis: Configuration and
893 performance of the data assimilation system, Quarterly Journal of the royal meteorological
894 society, 137, 553-597, 2011.

895 Dee, D. P., Uppala, S. M., Simmons, A., Berrisford, P., Poli, P., Kobayashi, S., Andrae, U.,
896 Balmaseda, M., Balsamo, G., and Bauer, d. P.: The ERA-Interim reanalysis: Configuration and
897 performance of the data assimilation system, Quarterly Journal of the royal meteorological
898 society, 137, 553-597, 2011.

899 Drobinski, P., Anav, A., Brossier, C. L., Samson, G., Stéfanon, M., Bastin, S., Baklouti, M.,
900 Béranger, K., Beuvier, J., and Bourdallé-Badie, R.: Model of the Regional Coupled Earth system
901 (MORCE): Application to process and climate studies in vulnerable regions, Environmental
902 Modelling & Software, 35, 1-18, 2012.

903 Dubois, C., Somot, S., Calmanti, S., Carillo, A., Déqué, M., Dell'Aquilla, A., Elizalde, A.,
904 Gualdi, S., Jacob, D., and L'hévéder, B.: Future projections of the surface heat and water budgets

https://doi.org/10.5194/gmd-2020-248
Preprint. Discussion started: 8 January 2021

of the Mediterranean Sea in an ensemble of coupled atmosphere–ocean regional climate models, Climate dynamics, 39, 1859-1884, 2012.

Fernández, V., Dietrich, D. E., Haney, R. L., and Tintoré, J.: Mesoscale, seasonal and interannual variability in the Mediterranean Sea using a numerical ocean model, Progress in Oceanography, 66, 321-340, 2005.

Forget, G., Campin, J.-M., Heimbach, P., Hill, C. N., Ponte, R. M., and Wunsch, C.: ECCO version 4: An integrated framework for non-linear inverse modeling and global ocean state estimation, 2015.

Forget, G., and Ferreira, D.: Global ocean heat transport dominated by heat export from the tropical Pacific, Nature Geoscience, 12, 351-354, 2019.

Furue, R., Jia, Y., McCreary, J. P., Schneider, N., Richards, K. J., Müller, P., Cornuelle, B. D., Avellaneda, N. M., Stammer, D., and Liu, C.: Impacts of regional mixing on the temperature structure of the equatorial Pacific Ocean. Part 1: Vertically uniform vertical diffusion, Ocean Modelling, 91, 91-111, 2015.

Giorgi, F.: Simulation of regional climate using a limited area model nested in a general circulation model, Journal of Climate, 3, 941-963, 1990.

Giorgi, F., Marinucci, M. R., and Bates, G. T.: Development of a second-generation regional climate model (RegCM2). Part I: Boundary-layer and radiative transfer processes, Monthly Weather Review, 121, 2794-2813, 1993.

Giorgi, F.: Climate change hot-spots, Geophysical research letters, 33, 2006.

Giorgi, F., Coppola, E., Solmon, F., Mariotti, L., Sylla, M., Bi, X., Elguindi, N., Diro, G., Nair, V., and Giuliani, G.: RegCM4: model description and preliminary tests over multiple CORDEX domains, Climate Research, 52, 7-29, 2012.

Giorgi, F., and Gutowski Jr, W. J.: Regional dynamical downscaling and the CORDEX initiative, Annual Review of Environment and Resources, 40, 467-490, 2015.

Giorgi, F., and Gutowski, W. J.: Coordinated experiments for projections of regional climate change, Current Climate Change Reports, 2, 202-210, 2016.

Giorgi, F.: Thirty years of regional climate modeling: where are we and where are we going next?, Journal of Geophysical Research: Atmospheres, 124, 5696-5723, 2019.

Grell, G. A.: Prognostic evaluation of assumptions used by cumulus parameterizations, Monthly weather review, 121, 764-787, 1993.

https://doi.org/10.5194/gmd-2020-248
Preprint. Discussion started: 8 January 2021

936 Grell, G. A., Dudhia, J., and Stauffer, D. R.: A description of the fifth-generation Penn
937 State/NCAR mesoscale model (MM5), 1994.

938 Hagemann, S., and Dümenil, L.: A parametrization of the lateral waterflow for the global scale,
939 Climate dynamics, 14, 17-31, 1997.

940 Hagemann, S., and Gates, L. D.: Validation of the hydrological cycle of ECMWF and NCEP
941 reanalyses using the MPI hydrological discharge model, Journal of Geophysical Research:
942 Atmospheres, 106, 1503-1510, 2001.

943 Heikkilä, U., Sandvik, A., and Sorteberg, A.: Dynamical downscaling of ERA-40 in complex
944 terrain using the WRF regional climate model, Climate dynamics, 37, 1551-1564, 2011.

945 Holte, J., Talley, L. D., Gilson, J., and Roemmich, D.: An Argo mixed layer climatology and
946 database, Geophysical Research Letters, 44, 5618-5626, 2017.

947 Hong, S.-Y., Dudhia, J., and Chen, S.-H.: A revised approach to ice microphysical processes for
948 the bulk parameterization of clouds and precipitation, Monthly weather review, 132, 103-120,
949 2004.

950 Hong, S.-Y., Noh, Y., and Dudhia, J.: A new vertical diffusion package with an explicit
951 treatment of entrainment processes, Monthly weather review, 134, 2318-2341, 2006.

952 Iacono, M. J., Delamere, J. S., Mlawer, E. J., Shephard, M. W., Clough, S. A., and Collins, W.
953 D.: Radiative forcing by long-lived greenhouse gases: Calculations with the AER radiative
954 transfer models, Journal of Geophysical Research: Atmospheres, 113, 2008.

955 Kain, J. S.: The Kain–Fritsch convective parameterization: an update, Journal of applied
956 meteorology, 43, 170-181, 2004.

957 Katragkou, E., García Díez, M., Vautard, R., Sobolowski, S. P., Zanis, P., Alexandri, G.,
958 Cardoso, R. M., Colette, A., Fernández Fernández, J., and Gobiet, A.: Regional climate hindcast
959 simulations within EURO-CORDEX: evaluation of a WRF multi-physics ensemble, 2015.

960 Kiehl, J., Hack, J., Bonan, G., Boville, B., and Briegleb, B.: Description of the NCAR
961 community climate model (CCM3). Technical Note, National Center for Atmospheric Research,
962 Boulder, CO (United States …, 1996.

963 Kotlarski, S., Keuler, K., Christensen, O. B., Colette, A., Déqué, M., Gobiet, A., Goergen, K.,
964 Jacob, D., Lüthi, D., and Van Meijgaard, E.: Regional climate modeling on European scales: a
965 joint standard evaluation of the EURO-CORDEX RCM ensemble, Geoscientific Model
966 Development, 7, 1297-1333, 2014.

https://doi.org/10.5194/gmd-2020-248
Preprint. Discussion started: 8 January 2021

967 Lascaratos, A., Williams, R. G., and Tragou, E.: A mixed-layer study of the formation of
968 Levantine Intermediate Water, Journal of Geophysical Research: Oceans, 98, 14739-14749,
969 1993.

970 Lascaratos, A., Roether, W., Nittis, K., and Klein, B.: Recent changes in deep water formation
971 and spreading in the eastern Mediterranean Sea: a review, Progress in oceanography, 44, 5-36,
972 1999.

973 Lebeaupin-Brossier, C., Bastin, S., Béranger, K., and Drobinski, P.: Regional mesoscale air–sea
974 coupling impacts and extreme meteorological events role on the Mediterranean Sea water
975 budget, Climate Dynamics, 44, 1029–1051, 2015.

976 Lermusiaux, P., and Robinson, A.: Features of dominant mesoscale variability, circulation
977 patterns and dynamics in the Strait of Sicily, Deep Sea Research Part I: Oceanographic Research
978 Papers, 48, 1953-1997, 2001.

979 Llasses, J., Jordà, G., Gomis, D., Adloff, F., Macías, D., Harzallah, A., Arsouze, T., Akthar, N.,
980 Li, L., and Elizalde, A.: Heat and salt redistribution within the Mediterranean Sea in the Med-
981 CORDEX model ensemble, Climate Dynamics, 51, 1119-1143, 2018.

982 Malanotte-Rizzoli, P., Manca, B. B., d'Alcala, M. R., Theocharis, A., Brenner, S., Budillon, G.,
983 and Ozsoy, E.: The Eastern Mediterranean in the 80s and in the 90s: the big transition in the
984 intermediate and deep circulations, Dynamics of Atmospheres and Oceans, 29, 365-395, 1999.

985 Mariotti, A., Struglia, M. V., Zeng, N., and Lau, K.: The hydrological cycle in the Mediterranean
986 region and implications for the water budget of the Mediterranean Sea, Journal of climate, 15,
987 1674-1690, 2002.

988 Marshall, J., Adcroft, A., Hill, C., Perelman, L., and Heisey, C.: A finite-volume,
989 incompressible Navier Stokes model for studies of the ocean on parallel computers, Journal of
990 Geophysical Research: Oceans, 102, 5753-5766, 1997.

991 Mertens, C., and Schott, F.: Interannual variability of deep-water formation in the Northwestern
992 Mediterranean, Journal of physical oceanography, 28, 1410-1424, 1998.

993 Millot, C., and Taupier-Letage, I.: Circulation in the Mediterranean sea, in: The Mediterranean
994 Sea, Springer, 29-66, 2005.

995 McKiver, W. J., Sannino, G., Braga, F., and Bellafiore, D.: Investigation of model capability in
996 capturing vertical hydrodynamic coastal processes: a case study in the north Adriatic Sea, Ocean
997 Sci., 12, 51-69, doi:10.5194/os-12-51-2016, 2016.

998 Mooney, P., Mulligan, F., and Fealy, R.: Evaluation of the sensitivity of the weather research and
999 forecasting model to parameterization schemes for regional climates of Europe over the period
1000 1990–95, Journal of Climate, 26, 1002-1017, 2013.

https://doi.org/10.5194/gmd-2020-248
Preprint. Discussion started: 8 January 2021

1001 Niu, G. Y., Yang, Z. L., Mitchell, K. E., Chen, F., Ek, M. B., Barlage, M., Kumar, A., Manning,
1002 K., Niyogi, D., and Rosero, E.: The community Noah land surface model with
1003 multiparameterization options (Noah-MP): 1. Model description and evaluation with
1004 local-scale measurements, Journal of Geophysical Research: Atmosp heres, 116, 2011.

1005 Omrani, H., Drobinski, P., and Dubos, T.: Using nudging to improve global-regional dynamic
1006 consistency in limited-area climate modeling: What should we nudge?, Climate Dynamics, 44,
1007 1627-1644, 2015.

1008 Onken, R., Robinson, A. R., Lermusiaux, P. F., Haley, P. J., and Anderson, L. A.: Data-driven
1009 simulations of synoptic circulation and transports in the Tunisia-Sardinia- Sicily region, Journal
1010 of Geophysical Research: Oceans, 108, 2003.

1011 Pal, J. S., Small, E. E., and Eltahir, E. A.: Simulation of regional-scale water and energy
1012 budgets: Representation of subgrid cloud and precipitation processes within RegCM, Journal of
1013 Geophysical Research: Atmospheres, 105, 29579-29594, 2000.

1014 Parras-Berrocal, I. M., Vazquez, R., Cabos, W., Sein, D., Mañanes, R., Perez-Sanz, J., and
1015 Izquierdo, A.: The climate change signal in the Mediterranean Sea in a regionally coupled
1016 atmosphere–ocean model, Ocean Science, 16, 743-765, 2020.

1017 Peng, Q., Xie, S.-P., Wang, D., Zheng, X.-T., and Zhang, H.: Coupled ocean-atmosphere
1018 dynamics of the 2017 extreme coastal El Niño, Nature communications, 10, 1-10, 2019.

1019 Pettenuzzo, D., Large, W., and Pinardi, N.: On the corrections of ERA-40 surface flux products
1020 consistent with the Mediterranean heat and water budgets and the connection between basin
1021 surface total heat flux and NAO, Journal of Geophysical Research: Oceans, 115, 2010.

1022 Pinardi, N., Arneri, E., Crise, A., Ravaioli, M., and Zavatarelli, M.: The physical, sedimentary
1023 and ecological structure and variability of shelf areas in the Mediterranean sea (27), The sea, 14,
1024 1243-1330, 2006.

1025 Pinardi, N., Zavatarelli, M., Adani, M., Coppini, G., Fratianni, C., Oddo, P., Simoncelli, S.,
1026 Tonani, M., Lyubartsev, V., and Dobricic, S.: Mediterranean Sea large-scale low-frequency
1027 ocean variability and water mass formation rates from 1987 to 2007: A retrospective analysis,
1028 Progress in Oceanography, 132, 318-332, 2015.

1029 Polkova, I., Köhl, A., and Stammer, D.: Impact of initialization procedures on the predictive skill
1030 of a coupled ocean–atmosphere model, Climate dynamics, 42, 3151-3169, 2014.

1031 Reale, M., Giorgi, F., Solidoro, C., Di Biagio, V., Di Sante, F., Mariotti, L., Farneti, R., and
1032 Sannino, G.: The Regional Earth System Model RegCM-ES: Evaluation of the Mediterranean
1033 climate and marine biogeochemistry, Journal of Advances in Modeling Earth Systems,
1034 e2019MS001812,

https://doi.org/10.5194/gmd-2020-248
Preprint. Discussion started: 8 January 2021

1035 Reynolds, R. W., Rayner, N. A., Smith, T. M., Stokes, D. C., and Wang, W.: An improved in situ
1036 and satellite SST analysis for climate, Journal of climate, 15, 1609-1625, 2002.

1037 Reynolds, R. W., Smith, T. M., Liu, C., Chelton, D. B., Casey, K. S., and Schlax, M. G.: Daily
1038 high-resolution-blended analyses for sea surface temperature, Journal of Climate, 20, 5473-5496,
1039 2007.

1040 Robinson, A., Sellschopp, J., Warn-Varnas, A., Leslie, W., Lozano, C., Haley Jr, P., Anderson,
1041 L., and Lermusiaux, P.: The Atlantic ionian stream, Journal of Marine Systems, 20, 129-156,
1042 1999.

1043 Roether, W., Manca, B. B., Klein, B., Bregant, D., Georgopoulos, D., Beitzel, V., Kovačević, V.,
1044 and Luchetta, A.: Recent changes in eastern Mediterranean deep waters, Science, 271, 333-335,
1045 1996.

1046 Roether, W., Klein, B., Manca, B. B., Theocharis, A., and Kioroglou, S.: Transient Eastern
1047 Mediterranean deep waters in response to the massive dense-water output of the Aegean Sea in
1048 the 1990s, Progress in Oceanography, 74, 540-571, 2007.

1049 Romanou, A., Tselioudis, G., Zerefos, C., Clayson, C., Curry, J., and Andersson, A.:
1050 Evaporation–precipitation variability over the Mediterranean and the Black Seas from satellite
1051 and reanalysis estimates, Journal of Climate, 23, 5268-5287, 2010.

1052 Rosso, I., Hogg, A. M., Kiss, A. E., and Gayen, B.: Topographic influence on submesoscale
1053 dynamics in the Southern Ocean, Geophysical Research Letters, 42, 1139-1147, 2015.

1054 Ruti, P. M., Somot, S., Giorgi, F., Dubois, C., Flaounas, E., Obermann, A., Dell'Aquila, A.,
1055 Pisacane, G., Harzallah, A., and Lombardi, E.: MED-CORDEX initiative for Mediterranean
1056 climate studies, Bulletin of the American Meteorological Society, 97, 1187-1208, 2016.

1057 Sanchez-Gomez, E., Somot, S., Josey, S., Dubois, C., Elguindi, N., and Déqué, M.: Evaluation of
1058 Mediterranean Sea water and heat budgets simulated by an ensemble of high resolution regional
1059 climate models, Climate dynamics, 37, 2067-2086, 2011.

1060 Sannino, G., Herrmann, M., Carillo, A., Rupolo, V., Ruggiero, V., Artale, V., and Heimbach, P.:
1061 An eddy-permitting model of the Mediterranean Sea with a two-way grid refinement at the Strait
1062 of Gibraltar, Ocean Modelling, 30, 56-72, 2009.

1063 Sannino, G., Carillo, A., Pisacane, G., and Naranjo, C.: On the relevance of tidal forcing in
1064 modelling the Mediterranean thermohaline circulation, Progress in oceanography, 134, 304-329,
1065 2015.

1066 Sannino, G., Sözer, A. & Özsoy, E. A high-resolution modelling study of the Turkish Straits
1067 System. Ocean Dynamics (2017) 67: 397. doi:10.1007/s10236-017-1039-2.

https://doi.org/10.5194/gmd-2020-248
Preprint. Discussion started: 8 January 2021


Geoscientific Model Development Discussions

1068 Schroeder, K., Ribotti, A., Borghini, M., Sorgente, R., Perilli, A., and Gasparini, G.: An
1069 extensive western Mediterranean deep water renewal between 2004 and 2006, Geophysical
1070 Research Letters, 35, 2008.

1071 Sevault, F., Somot, S., Alias, A., Dubois, C., Lebeaupin-Brossier, C., Nabat, P., Adloff, F.,
1072 Déqué, M., and Decharme, B.: A fully coupled Mediterranean regional climate system model:
1073 design and evaluation of the ocean component for the 1980–2012 period, Tellus A: Dynamic
1074 Meteorology and Oceanography, 66, 23967, 2014.

1075 Sitz, L., Di Sante, F., Farneti, R., Fuentes-Franco, R., Coppola, E., Mariotti, L., Reale, M.,
1076 Sannino, G., Barreiro, M., and Nogherotto, R.: Description and evaluation of the E arth S ystem
1077 Regional Climate M odel (R eg CM-ES), Journal of Advances in Modeling Earth Systems, 9,
1078 1863-1886, 2017.

1079 Skamarock, W. C., and Klemp, J. B.: A time-split nonhydrostatic atmospheric model for weather
1080 research and forecasting applications, Journal of computational physics, 227, 3465-3485, 2008.

1081 Somot, S., Sevault, F., Déqué, M., and Crépon, M.: 21st century climate change scenario for the
1082 Mediterranean using a coupled atmosphere–ocean regional climate model, Global and Planetary
1083 Change, 63, 112-126, 2008.

1084 Somot, S., Houpert, L., Sevault, F., Testor, P., Bosse, A., Taupier-Letage, I., Bouin, M.-N.,
1085 Waldman, R., Cassou, C., and Sanchez-Gomez, E.: Characterizing, modelling and understanding
1086 the climate variability of the deep water formation in the North-Western Mediterranean Sea,
1087 Climate Dynamics, 51, 1179-1210, 2018.

1088 Somot, S., Ruti, P., Ahrens, B., Coppola, E., Jordà, G., Sannino, G., Solmon, F. Editorial for the
1089 Med-CORDEX special issue (2018) Climate Dynamics, 51 (3), pp. 771-777.

1090 Stammer, D., Wunsch, C., Giering, R., Eckert, C., Heimbach, P., Marotzke, J., Adcroft, A., Hill,
1091 C., and Marshall, J.: Volume, heat, and freshwater transports of the global ocean circulation
1092 1993–2000, estimated from a general circulation model constrained by World Ocean Circulation
1093 Experiment (WOCE) data, Journal of Geophysical Research: Oceans, 108, 7-1-7-23, 2003.

1094 Sun, R., Subramanian, A. C., Miller, A. J., Mazloff, M. R., Hoteit, I., and Cornuelle, B. D.:
1095 SKRIPS v1. 0: A regional coupled ocean-atmosphere modeling framework (MITgcm-WRF)
1096 using ESMF/NUOPC, description and preliminary results for the Red Sea, 2019.

1097 Theocharis, A., Nittis, K., Kontoyiannis, H., Papageorgiou, E., and Balopoulos, E.: Climatic
1098 changes in the Aegean Sea influence the Eastern Mediterranean thermohaline circulation (1986–
1099 1997), Geophysical Research Letters, 26, 1617-1620, 1999.

1100 Theocharis, A., Klein, B., Nittis, K., and Roether, W.: Evolution and status of the Eastern
1101 Mediterranean Transient (1997–1999), Journal of Marine Systems, 33, 91-116, 2002.

https://doi.org/10.5194/gmd-2020-248
Preprint. Discussion started: 8 January 2021

1102 Tuel, A., and Eltahir, E.: Why Is the Mediterranean a Climate Change Hot Spot?, Journal of
1103 Climate, 33, 5829-5843, 2020.

1104 Turuncoglu, U. U., and Sannino, G.: Validation of newly designed regional earth system model
1105 (RegESM) for Mediterranean Basin, Climate dynamics, 48, 2919-2947, 2017.

1106 Turuncoglu, U. U.: Toward modular in situ visualization in Earth system models: the regional
1107 modeling system RegESM 1.1, Geoscientific Model Development, 12, 2019.

1108 Vervatis, V. D., Sofianos, S. S., Skliris, N., Somot, S., Lascaratos, A., and Rixen, M.:
1109 Mechanisms controlling the thermohaline circulation pattern variability in the Aegean–Levantine
1110 region. A hindcast simulation (1960–2000) with an eddy resolving model, Deep Sea Research
1111 Part I: Oceanographic Research Papers, 74, 82-97, 2013.

1112 Waldron, K. M., Paegle, J., and Horel, J. D.: Sensitivity of a spectrally filtered and nudged
1113 limited-area model to outer model options, Monthly weather review, 124, 529-547, 1996.

1114 Wu, P., Haines, K., and Pinardi, N.: Toward an understanding of deep-water renewal in the
1115 eastern Mediterranean, Journal of Physical Oceanography, 30, 443-458, 2000.

1116 Zavatarielli, M., and Mellor, G. L.: A numerical study of the Mediterranean Sea circulation,
1117 Journal of Physical Oceanography, 25, 1384-1414, 1995.

1118

1119

1120

1121

1122

1123

https://doi.org/10.5194/gmd-2020-248
Preprint. Discussion started: 8 January 2021

Geoscientific Model Development Discussions

TABLES

Table 1. Set up of atmospheric components of the ENEA-REG system with main physical parameterizations adopted in the simulations.

Model set-up	**WRF**	**RegCM**
Domain	Med-CORDEX	Med-CORDEX
Simulation period	1st October 1979-31st December 2013	1st October 1979-31st December 2013
Horizontal resolution	15 km	20 km
Vertical resolution	35 levels up to 50 hPa	23 levels up to 50 hPa
Domain size	350x280 (lon x lat)	350x250 (lon x lat)
Physical option	**Adopted schemes**	**Adopted schemes**
Microphysics	WSM5 (single-moment 5 class)	SUBEX
Cumulus parameterization	Kain-Fritsch	Grell
Shortwave radiation	RRTMG	CCM3
Longwave radiation	RRTMG	CCM3
Land-surface	Noah-MP	BATS
Planetary boundary layer	Yonsei University Scheme	UW-PBL
Surface layer	Revised MM5 Monin-Obukhov scheme	Zeng
Boundary condition	**Configuration**	**Configuration**
Meteorological boundary	ERA-Interim (~75 km), 6h	ERA-Interim (~75 km), 6h
Relaxation zone	10 points, exponential	6 points, exponential
Nudging	Spectral	N/A

https://doi.org/10.5194/gmd-2020-248
Preprint. Discussion started: 8 January 2021

Geoscientific Model Development Discussions
Open Access
EGU

1138 **Table 2.** Mean annual water transport (in *Sv*) through the two main straits of Mediterranean Sea
1139 over the period 1982–2013.

	Gibraltar			Sicily		
	Eastward	Westward	Net	Northward	Southward	Net
WRF- MITgcm	0.965	-0.905	0.061	1.332	-1.357	-0.025
RegCM- MITgcm	1.009	-0.947	0.063	1.326	-1.356	-0.030

1140
1141 .
1142
1143
1144
1145
1146
1147
1148
1149
1150
1151
1152
1153
1154
1155
1156
1157
1158
1159
1160
1161
1162
1163
1164
1165
1166
1167
1168
1169
1170
1171
1172
1173
1174

https://doi.org/10.5194/gmd-2020-248
Preprint. Discussion started: 8 January 2021

Geoscientific Model Development Discussions

Table 3. Averaged temperature (°*C*) and salinity (*psu*) at different depths for the DIVA dataset and anomalies computed between the reference DIVA data and results from the coupled models. Values are averaged over the entire Mediterranean Sea and over the western and eastern basins for the temporal period 1982–2013.

		Temperature				**Salinity**			
		Depth [m]				Depth [m]			
		0-150	**150-600**	**600-3500**	**0-3500**	**0-150**	**150-600**	**600-3500**	**0-3500**
MED	**DIVA**	16.20	14.04	13.33	13.78	38.43	38.73	38.62	38.63
	WRF	-0.24	0.08	0.12	0.06	-0.01	0.02	0.08	0.06
	RegCM	-0.88	-0.39	0.03	-0.17	-0.01	-0.02	0.10	0.06
WMED	**DIVA**	14.99	13.42	12.98	13.26	37.95	38.51	38.47	38.43
	WRF	0.13	0.15	0.05	0.07	-0.08	-0.03	0.01	-0.01
	RegCM	-0.40	-0.28	-0.05	-0.13	-0.07	-0.08	0.01	-0.02
EMED	**DIVA**	16.89	14.41	13.56	14.10	38.70	38.86	38.73	38.75
	WRF	-0.45	-0.04	0.15	0.03	0.03	0.06	0.10	0.09
	RegCM	-1.16	-0.44	0.05	-0.20	0.02	0.02	0.13	0.10

https://doi.org/10.5194/gmd-2020-248
Preprint. Discussion started: 8 January 2021

Geoscientific Model Development Discussions

1192

1193 **FIGURES**

1194

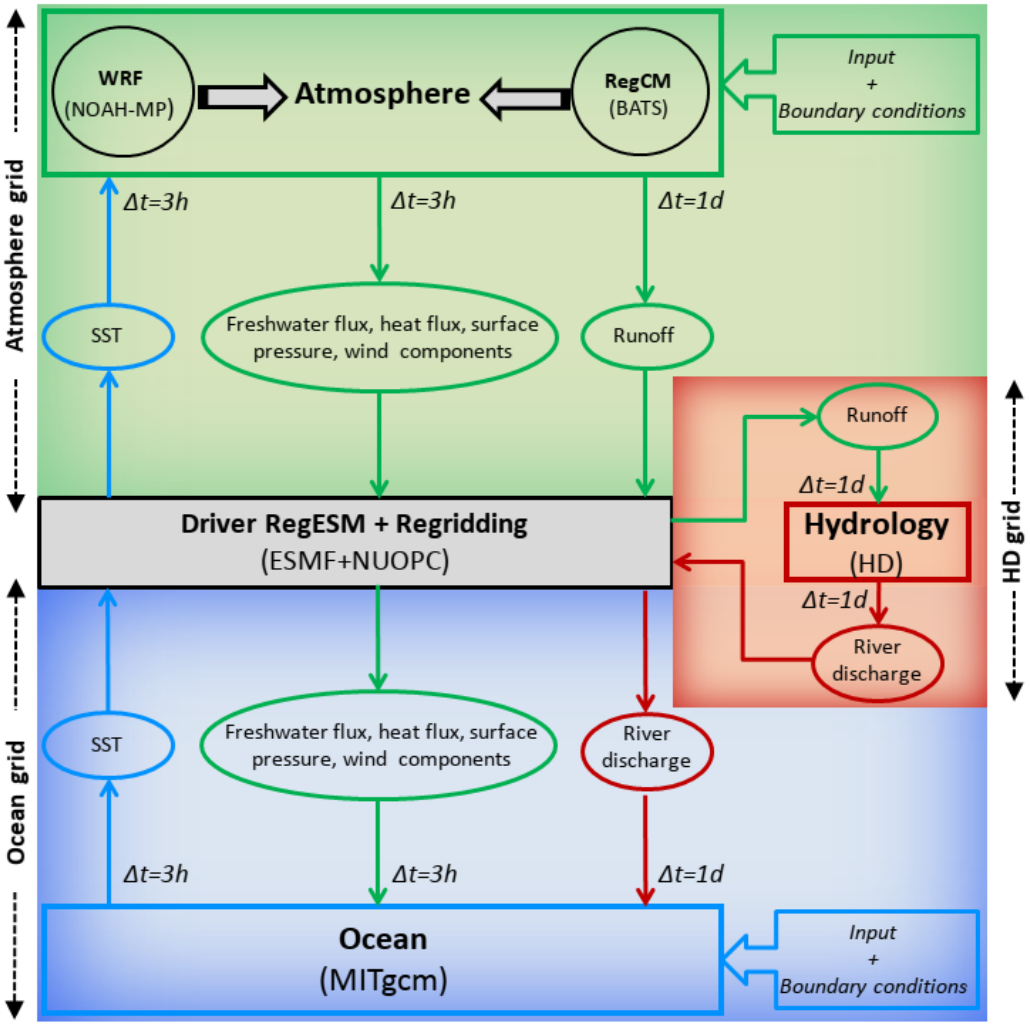

1195

1196 **Figure 1.** Schematic description of the ENEA-REG regional coupled model. The green block
1197 represents the atmosphere with the two components that can be selected and used (i.e. WRF and
1198 RegCM), the blue block is the ocean component (i.e. MITgcm), the red block represents the river
1199 routing component while the grey block is the ESMF/NUOPC coupler which collects, regrids
1200 and exchanges variables between the different components of the system.

https://doi.org/10.5194/gmd-2020-248
Preprint. Discussion started: 8 January 2021

Geoscientific Model Development Discussions
Open Access
EGU

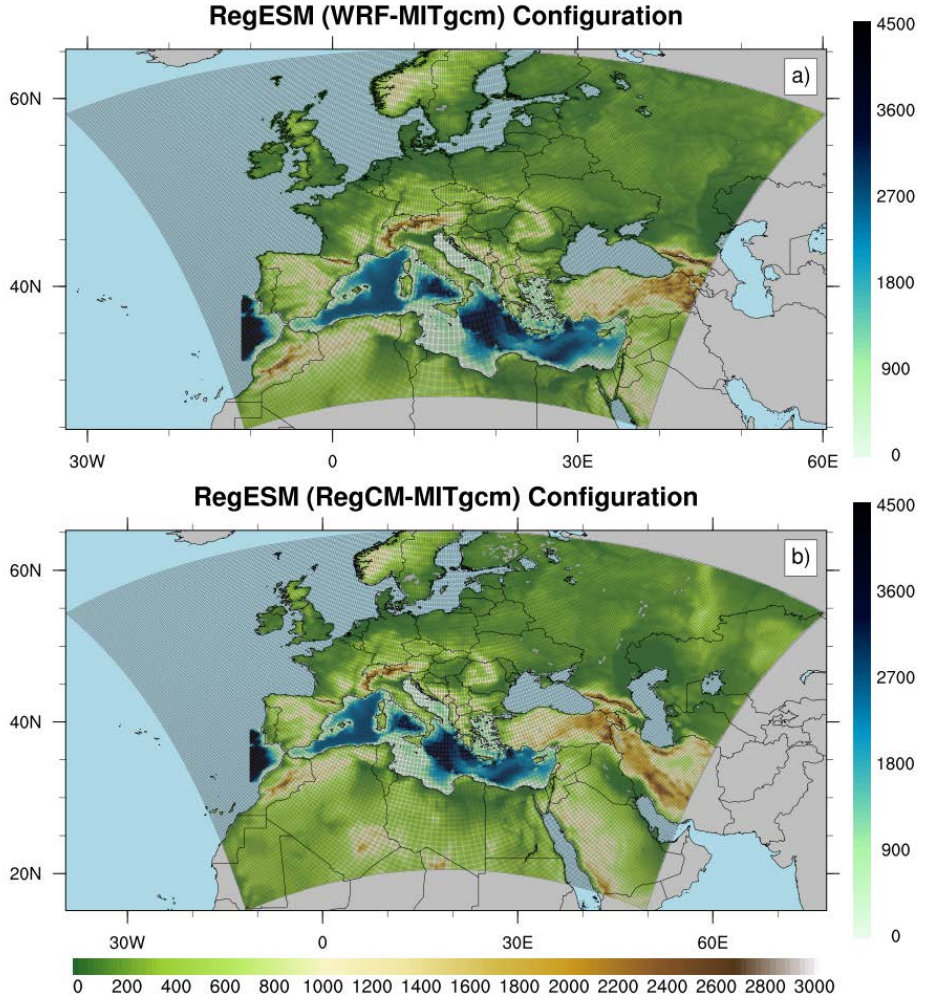

Figure 2. Different domains of the ENEA-REG system, with green shading representing the topography of the atmospheric models (i.e. WRF and RegCM, solid grey lines indicate the computational domain) and blue shading the bathymetry of the ocean component.

https://doi.org/10.5194/gmd-2020-248
Preprint. Discussion started: 8 January 2021

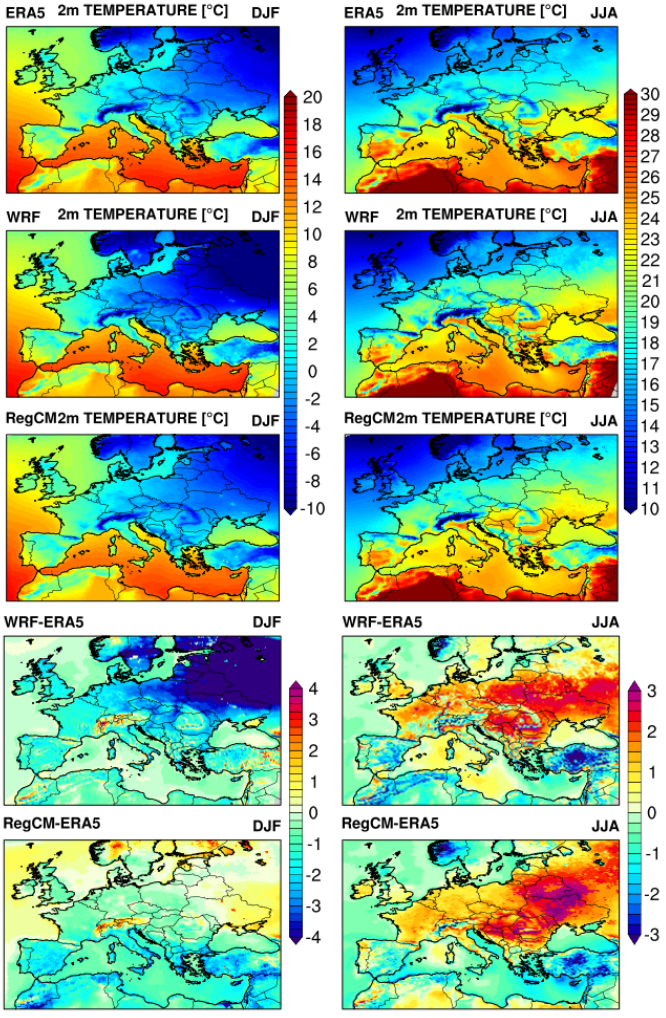

Figure 3. Seasonal winter (DJF) and summer (JJA) spatial pattern (upper three panels) and bias (lower two panels) of 2m air temperature as simulated by the coupled model using the two atmospheric components (i.e. WRF and RegCM) and ERA5 dataset between 1982 and 2013. Note that in the bias panels ERA5 data are interpolated into the atmospheric model grid. Mind also the differences in colour scales between DJF and JJA climatologies.

https://doi.org/10.5194/gmd-2020-248
Preprint. Discussion started: 8 January 2021

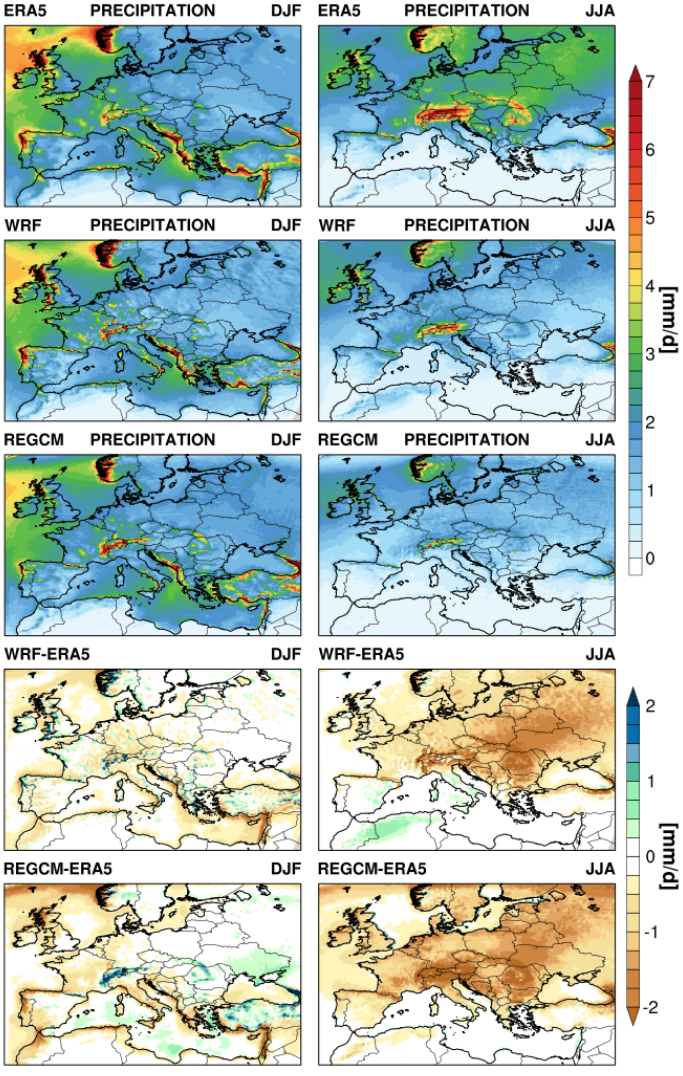

Figure 4. Seasonal winter (DJF) and summer (JJA) spatial pattern (upper three panels) and bias (lower two panels) of precipitation as simulated by the coupled model using the two atmospheric components (i.e. WRF and RegCM) and ERA5 dataset between 1982 and 2013. Note that in the bias panels ERA5 data are interpolated into the atmospheric model grid.

https://doi.org/10.5194/gmd-2020-248
Preprint. Discussion started: 8 January 2021

Geoscientific Model Development Discussions

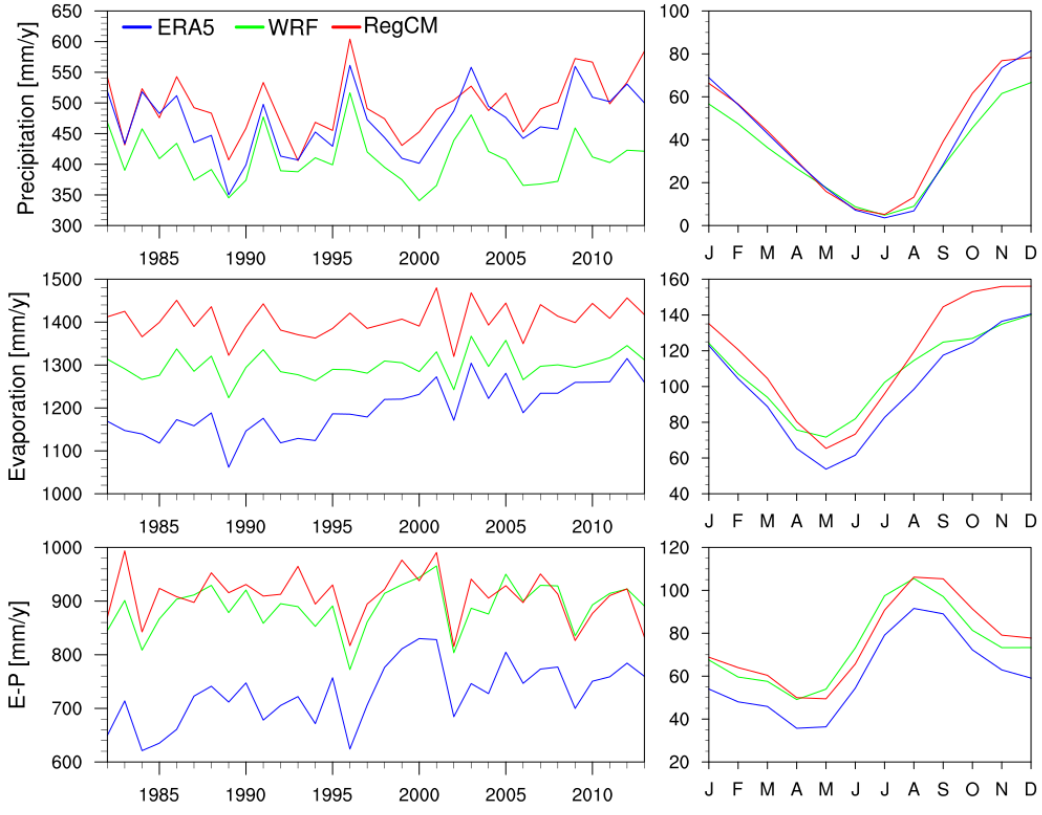

Figure 5. Interannual variability (left panels) and mean seasonal cycle (right panels, units mm/month) of freshwater flux components. i.e. precipitation (P), evaporation (E) and their difference (E-P), computed over the Mediterranean basin as simulated by the ENEA-REG system and ERA5 reanalysis.

https://doi.org/10.5194/gmd-2020-248
Preprint. Discussion started: 8 January 2021

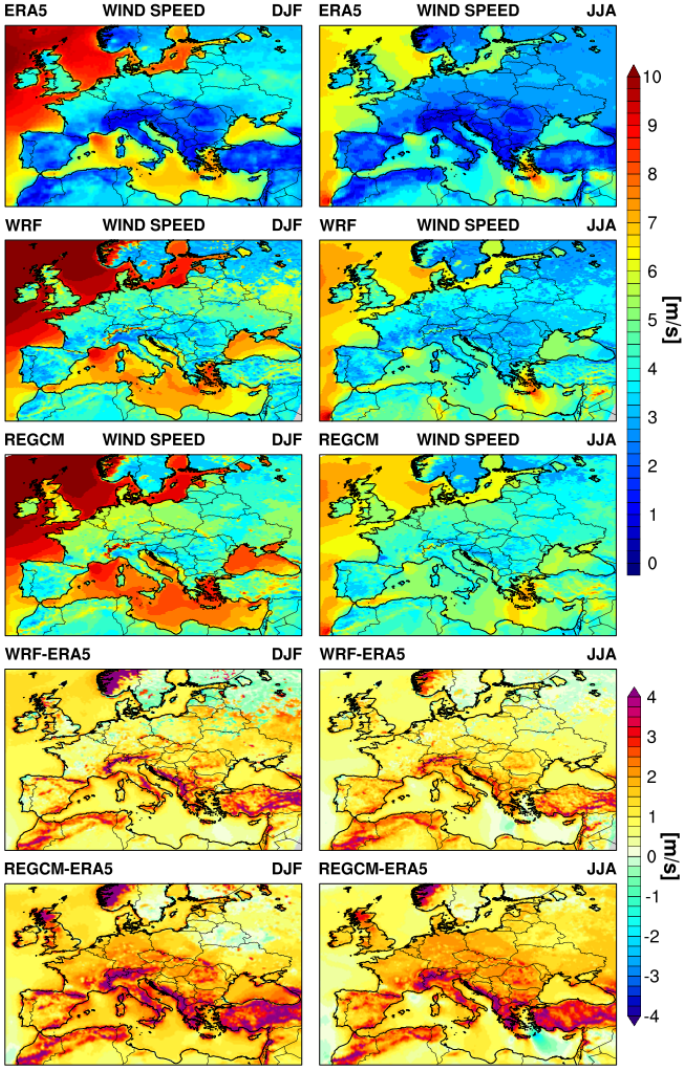

Figure 6. Seasonal winter (DJF) and summer (JJA) spatial pattern (upper three panels) and bias (lower two panels) of 10m wind speed as simulated by the coupled model using the two atmospheric components (i.e. WRF and RegCM) and ERA5 dataset between 1982 and 2013. Note that in the bias panels ERA5 data are interpolated into the atmospheric model grid.

https://doi.org/10.5194/gmd-2020-248
Preprint. Discussion started: 8 January 2021

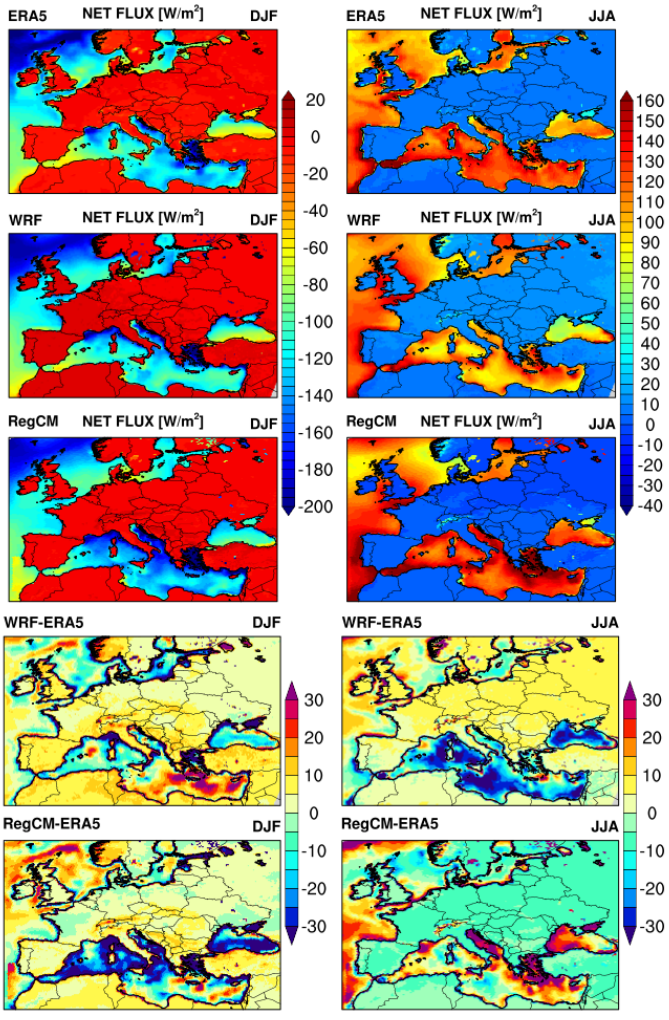

Figure 7. Seasonal winter (DJF) and summer (JJA) spatial pattern (upper three panels) and bias (lower two panels) of net heat flux as simulated by the coupled model using the two atmospheric components (i.e. WRF and RegCM) and ERA5 dataset between 1982 and 2013. Note that ERA5 data are interpolated into atmospheric model grids for comparison purposes. Mind also the differences in colour scales between DJF and JJA climatologies.

https://doi.org/10.5194/gmd-2020-248
Preprint. Discussion started: 8 January 2021

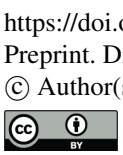

Geoscientific Model Development Discussions

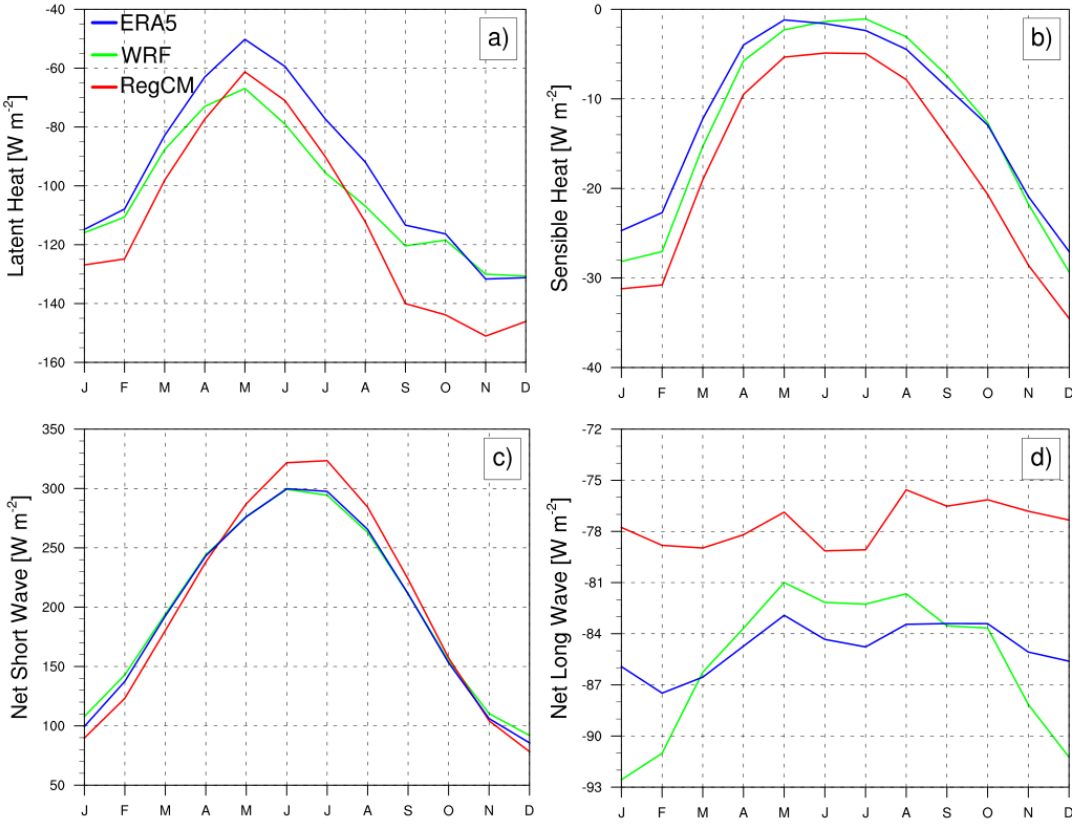

1236

1237 **Figure 8.** Mean seasonal cycle of net heat flux components over the Mediterranean basin as
1238 simulated by the ENEA-REG system and ERA5 reanalysis over the period 1982-2013.

https://doi.org/10.5194/gmd-2020-248
Preprint. Discussion started: 8 January 2021

Geoscientific Model Development Discussions

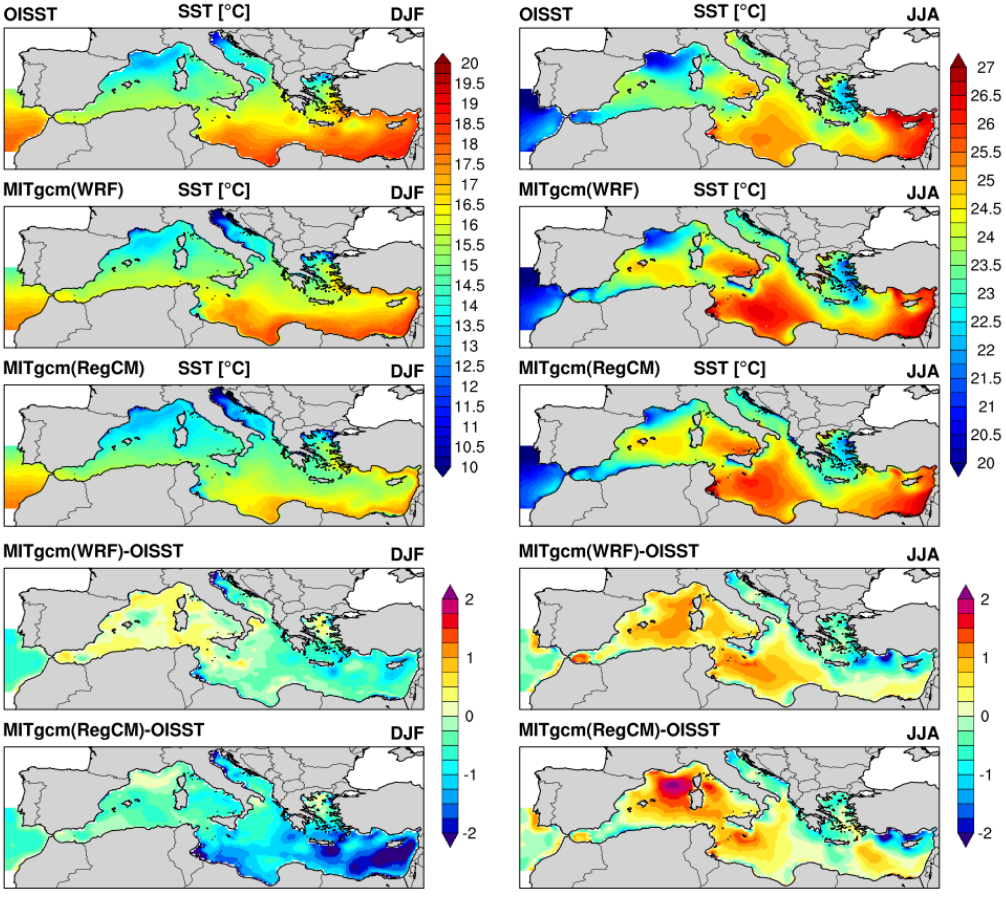

1239

1240 **Figure 9.** Seasonal winter (DJF) and summer (JJA) spatial pattern (upper three panels) and bias
1241 (lower two panels) of sea surface temperature (SST [°C]) as simulated by the coupled model
1242 using the two atmospheric components as forcing (i.e. WRF and RegCM) and OISST dataset
1243 between 1982 and 2013. Note that OISST data are interpolated into ocean model grid for
1244 comparison purposes. Mind also the differences in colour scales between DJF and JJA
1245 climatologies.

1246

https://doi.org/10.5194/gmd-2020-248
Preprint. Discussion started: 8 January 2021

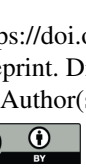

Geoscientific Model Development Discussions
Open Access
EGU

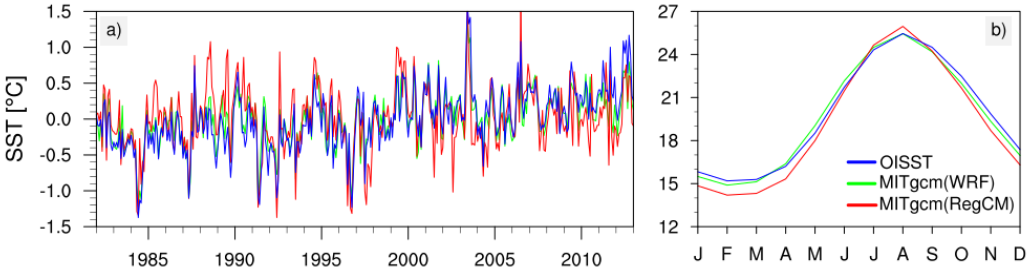

Figure 10. Comparison of monthly anomalies (left panel) and mean seasonal cycles (right panel) of sea surface temperature simulated by the ENEA-REG system with OISST observation.

https://doi.org/10.5194/gmd-2020-248
Preprint. Discussion started: 8 January 2021

Geoscientific Model Development Discussions

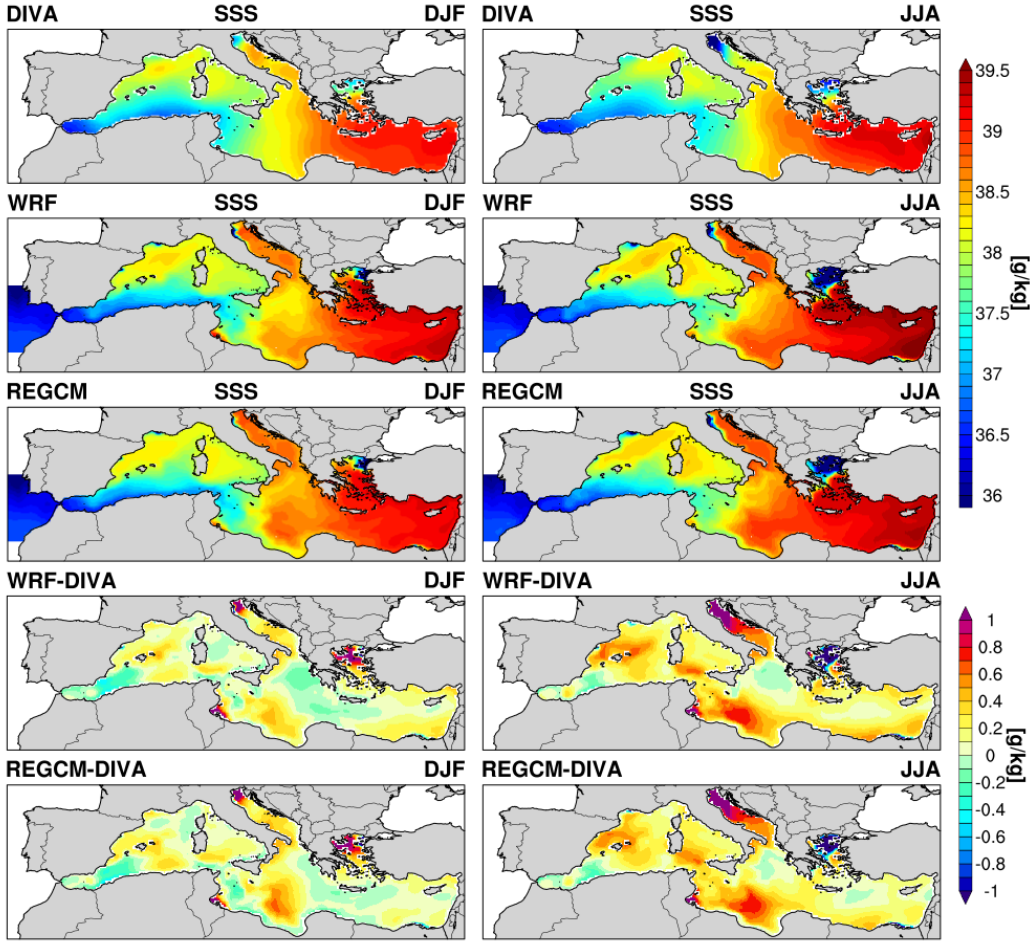

Figure 11. Seasonal winter (DJF) and summer (JJA) spatial pattern (upper three panels) and bias (lower two panels) of sea surface salinity (SSS [*g/kg*]) as simulated by the coupled model using the two atmospheric components (i.e. WRF and RegCM) and DIVA dataset between 1982 and 2013. Note that DIVA data are interpolated into ocean model grid for comparison purposes.

https://doi.org/10.5194/gmd-2020-248
Preprint. Discussion started: 8 January 2021

Geoscientific Model Development Discussions
Open Access
EGU

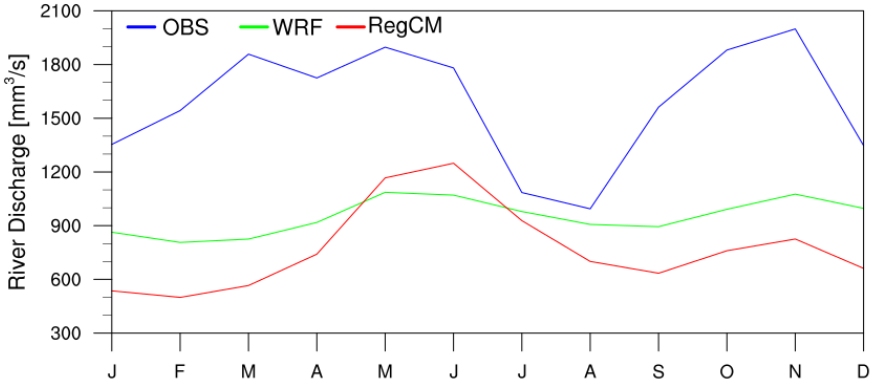

Figure 12. Mean seasonal cycle of the river discharge of the Po river into the Adriatic Sea as simulated by the two configurations of the coupled model and the observational dataset RivDis.

https://doi.org/10.5194/gmd-2020-248
Preprint. Discussion started: 8 January 2021

Geoscientific Model Development Discussions
Open Access
EGU

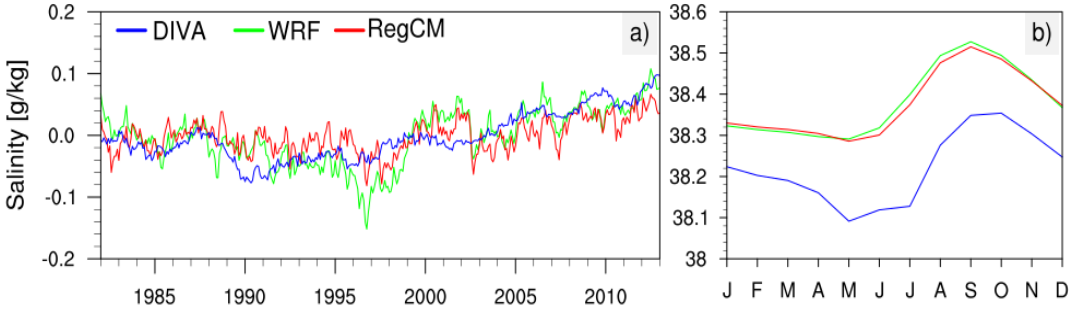

1277

1278 **Figure 13.** Comparison of monthly anomalies (left panel) and mean seasonal cycles (right panel)
1279 of sea surface salinity simulated by the ENEA-REG system with DIVA dataset.

1280

1281

https://doi.org/10.5194/gmd-2020-248
Preprint. Discussion started: 8 January 2021

Geoscientific Model Development Discussions

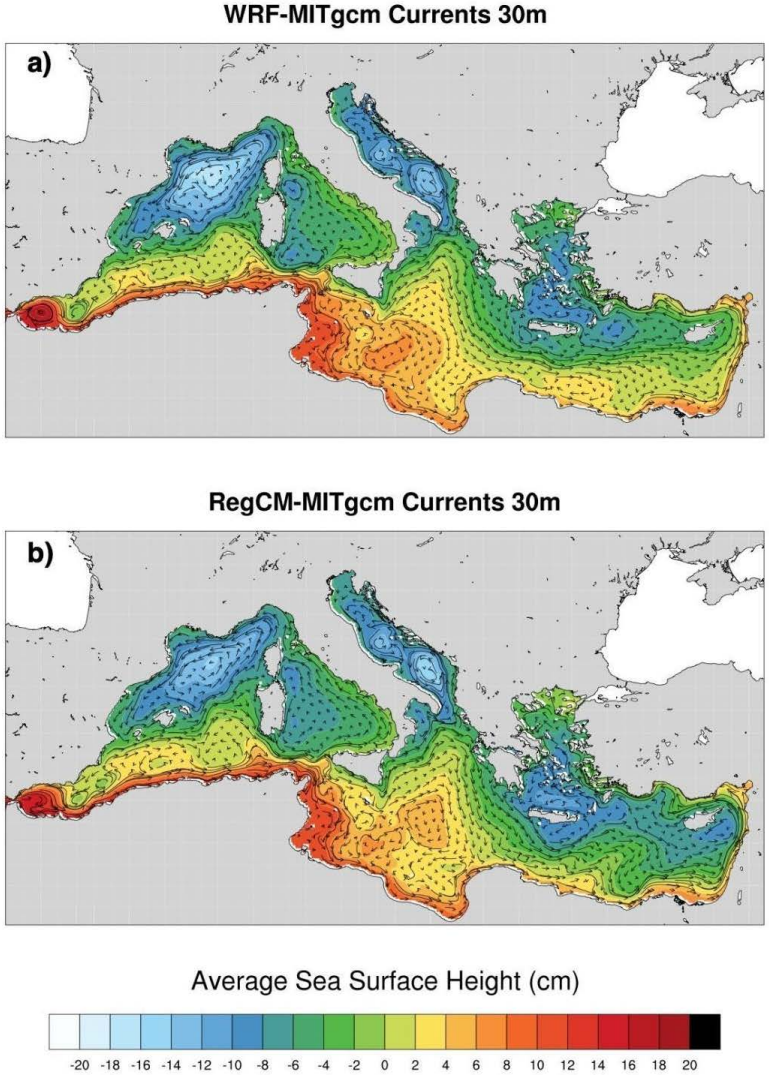

Figure 14. Mean annual sea surface elevation along with sub-surface (30m) circulation as simulated by the two configurations of the coupled atmosphere-ocean model; data are averaged over the temporal period 1982-2013.

https://doi.org/10.5194/gmd-2020-248
Preprint. Discussion started: 8 January 2021

Geoscientific Model Development Discussions
Open Access
EGU

1292

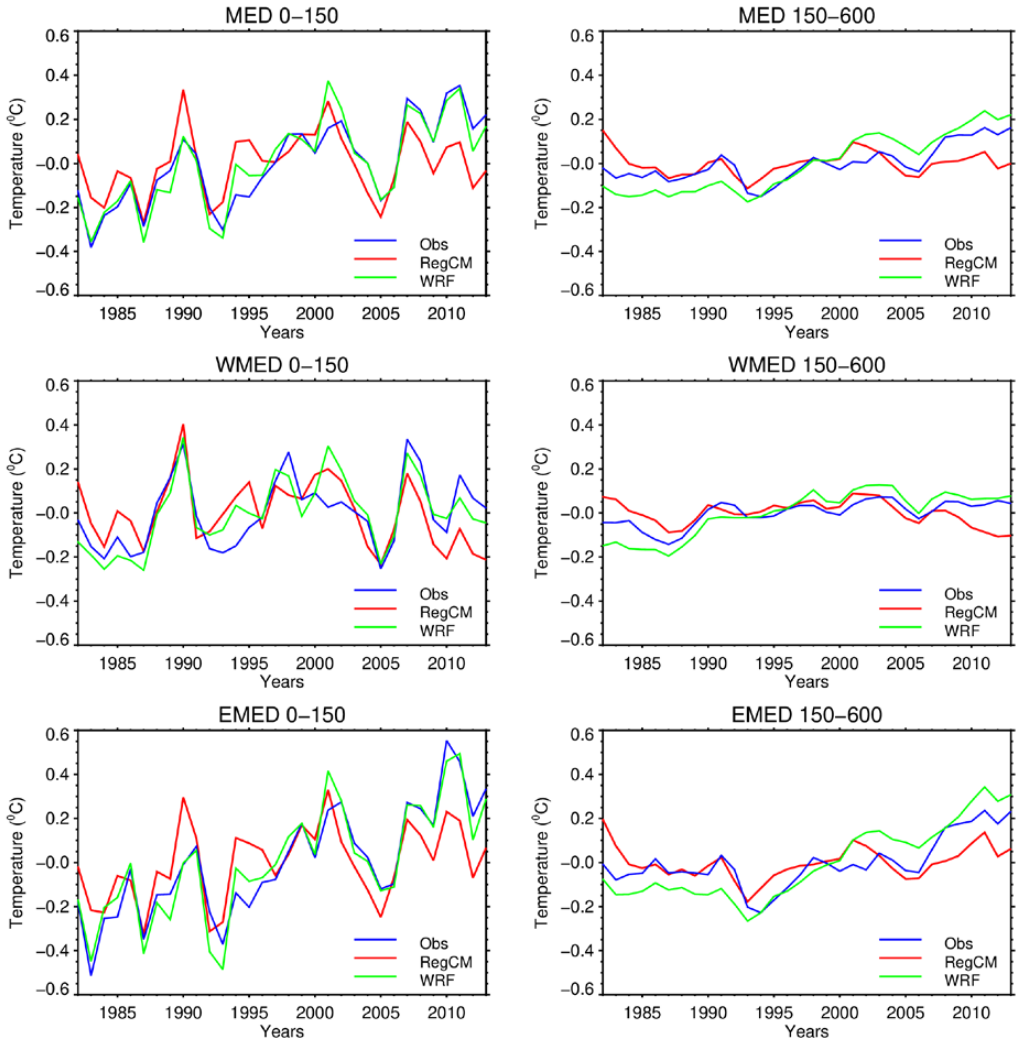

1293
1294 **Figure 15.** Annual mean temperature anomalies (°*C*) for upper (0-150 m) and intermediate (150-
1295 600 m) layers of the Mediterranean Sea, Western and Eastern basins over the period 1982-2013.

https://doi.org/10.5194/gmd-2020-248
Preprint. Discussion started: 8 January 2021

Geoscientific Model Development Discussions

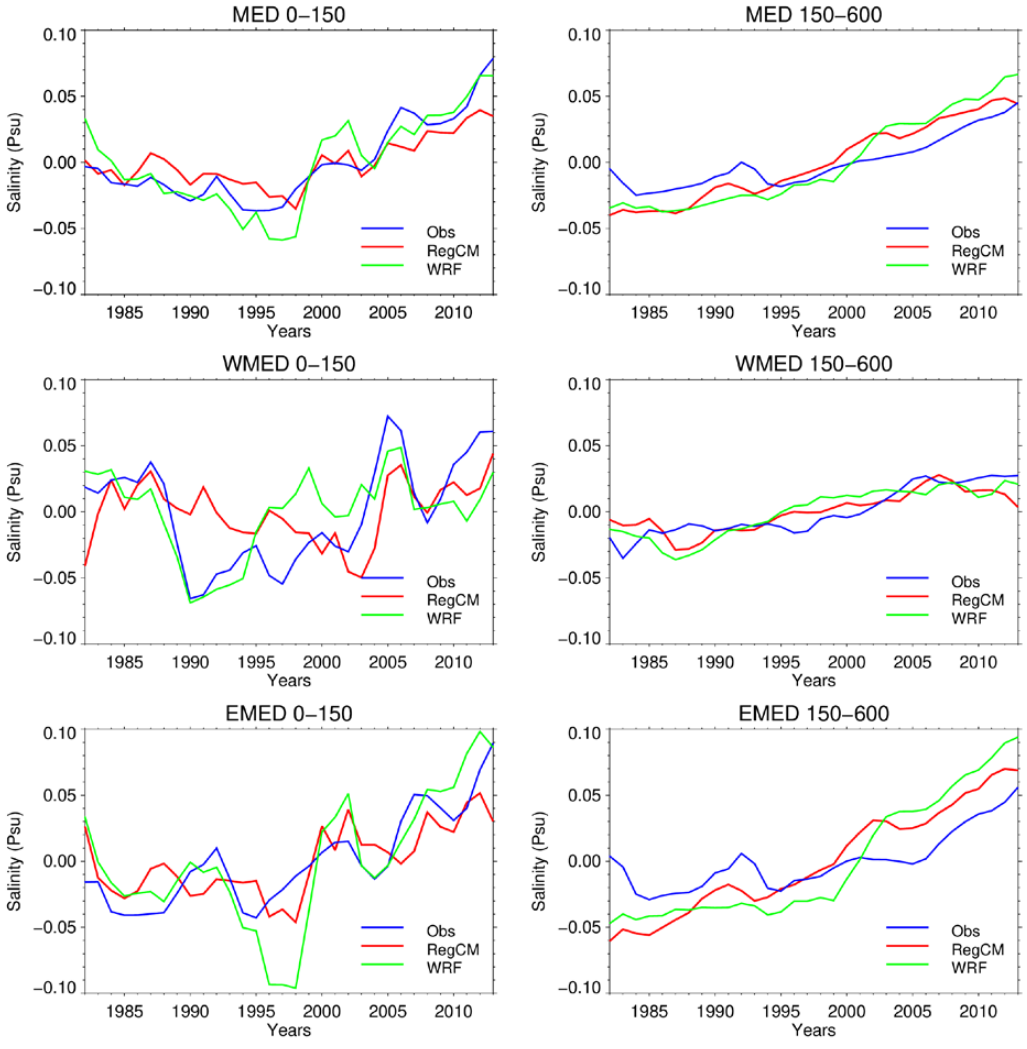

Figure 16. Annual mean salinity anomalies (*psu*) for upper (0-150 m) and intermediate (150-600 m) layers of the Mediterranean Sea, Western and Eastern basins over the period 1982-2013.

https://doi.org/10.5194/gmd-2020-248
Preprint. Discussion started: 8 January 2021

Geoscientific Model Development Discussions
Open Access
EGU

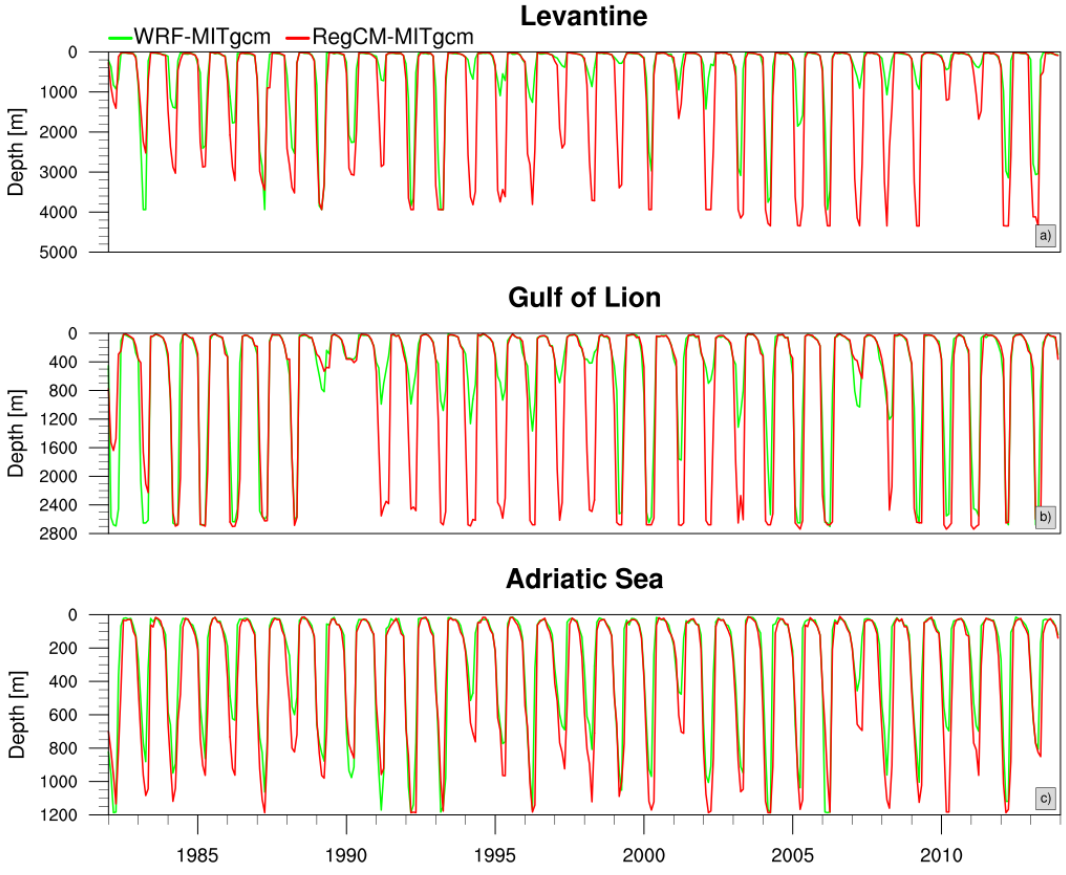

Figure 17. Time evolution of the maximum MLD computed over the Levantine basin, Gulf of Lion area and Adriatic Sea for WRF-MITgcm (green) and RegCM-MITgcm (red) simulations.

https://doi.org/10.5194/gmd-2020-248
Preprint. Discussion started: 8 January 2021

Geoscientific Model Development Discussions

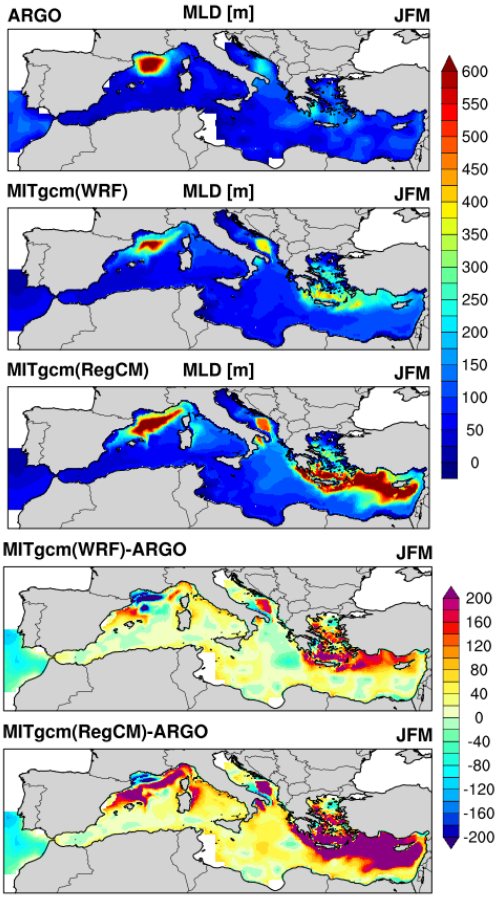

1307

1308 **Figure 18.** Winter (JFM) spatial pattern (upper three panels) and bias (lower two panels) of
1309 mixed layer depth (MLD [*m*]) as simulated by the coupled model using the two atmospheric
1310 components as forcing (i.e. WRF and RegCM) and ARGO dataset between 1982 and 2013. Note
1311 that ARGO data are interpolated into the ocean model grid for comparison purposes.

https://doi.org/10.5194/gmd-2020-248
Preprint. Discussion started: 8 January 2021

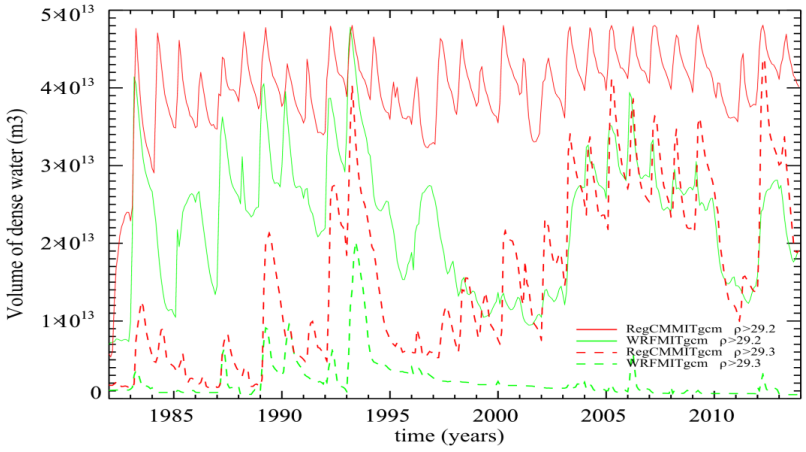

Figure 19. Monthly volume of water denser than 29.2 kg m^{-3} (solid line) and denser than 29.3 kg m^{-3} (dashed line) produced in the Cretan Sea for the two configurations of ENEA-REG system.